

# Glueball-Quarkonium Mixing in the Quark and Chromon Model

Pengming Zhang,<sup>1</sup> Li-Ping Zou,<sup>1,2</sup> Ju-Jun Xie,<sup>1</sup> J. H. Yoon,<sup>3</sup> and Y. M. Cho<sup>4,5,\*</sup>

<sup>1</sup>*Institute of Modern Physics, Chinese Academy of Science, Lanzhou 730000, China*

<sup>2</sup>*Institute of Basic Sciences, Konkuk University, Seoul 143-701, Korea*

<sup>3</sup>*Department of Physics, Konkuk University, Seoul 143-701, Korea*

<sup>4</sup>*Administration Building 310-4, Konkuk University, Seoul 143-701, Korea*

<sup>5</sup>*School of Physics and Astronomy, Seoul National University, Seoul 151-747, Korea*

(Dated: October 25, 2016)

The Abelian decomposition of QCD which decomposes the gluons to the color neutral binding gluons (the neurons and the monopoles) and the colored valence gluons (the chromons) gauge independently naturally generalizes the quark model to the quark and chromon model which can play the central role in hadron spectroscopy. We discuss how the quark and chromon model describes the glueballs and the glueball-quarkonium mixing in QCD. We present the numerical analysis of glueball-quarkonium mixing in  $0^{++}$ ,  $2^{++}$ , and  $0^{-+}$  sectors below 2 GeV, and show that in the  $0^{++}$  sector  $f_0(500)$  and  $f_0(1500)$ , in the  $2^{++}$  sector  $f_2(1950)$ , and in the  $0^{-+}$  sector  $\eta(1405)$  and  $\eta(1475)$  could be identified as predominantly the glueball states. We discuss the physical implications of our result.

PACS numbers: 11.15.-q, 12.38.Aw, 12.39.MK, 14.70.Dj

Keywords: binding gluon, valence gluon, constituent gluon, neuron, chromon, quark and chromon model, glueball, neuroball, chromoball, glueball-quarkonium mixing.

## I. INTRODUCTION

An important issues in hadron spectroscopy is the identification of the glueballs. The general wisdom is that QCD must have the glueballs made of gluons [1–3]. According to the model-independent definition, the glueballs are the bound states of (confined) gluons. Several models of glueballs have been proposed to explain how to construct them [4–9]. And the lattice QCD was able to construct the low-lying glueballs based on the first principles of QCD dynamics [10, 11]. Moreover, huge efforts have been made to identify the glueballs experimentally and theoretically [12–16]. And Particle Data Group (PDG) has accumulated a large number of hadronic states which do not seem to fit to the simple quark model as the glueball candidates [17].

But the search for the glueballs has not been so successful for two reasons. First, theoretically there has been no consensus on how to construct the glueballs. This has made it difficult to predict what kind of glueballs we could expect. To see this consider the two leading models of glueballs, the bag model and the constituent gluon model.

The bag model proposes to identify the glueballs as the confined gluon fields in a bag [4, 5]. According to this model the glueballs are made of infinite number of

gluons, so that there are no constituent gluons (i.e., a finite number of gluons) which make up the glueballs. Unfortunately the model does not tell much about the role of gluons in the glueball spectroscopy, except that they are confined in a bag.

On the other hand in the constituent model the glueballs are identified as the bound states of a finite number of the color octet “constituent gluons” [7, 8]. Intuitively this model looks very attractive. But obviously we need the gluon field to bind them, so that we need an infinite number of binding gluons as well as a finite number of constituent gluons to make a glueball. Unfortunately, this model does not tell what is the difference between the constituent gluons and the binding gluons.

The other reason is that it is not clear how to identify the glueballs experimentally. This is partly because the glueballs could mix with quarkonia, so that we must take care of the possible mixing to identify the glueballs experimentally [12–16]. This is why we have very few candidates of the glueballs so far, compared to huge hadron spectrum made of quarks listed by PDG.

This makes the search for the glueballs an urgent issue in high energy physics. Indeed, GlueX at Jefferson Lab and PANDA at FAIR are specifically designed to search for the glueballs [18, 19]. To have a successful identification of glueballs, however, we must have a better picture of the glueballs.

The Abelian decomposition of QCD helps us to do that [20–23]. It decomposes the QCD gauge potential to the color neutral restricted potential which has the

---

\*Electronic address: ymcho7@konkuk.ac.kr

full color gauge degrees of freedom and the colored valence potential which transforms gauge covariantly in a gauge independent way. This tells that there are two types of gluons which play different roles. The restricted potential describes the binding gluons which bind the colored source, while the valence potential describes the constituent gluons (the chromons) which become the colored source of QCD. So we can view QCD as the restricted QCD (RCD) made of the binding gluons which has the chromons as the colored source. This is against the common wisdom that all gluons (because of the gauge symmetry) are the same, carrying the same color charge. The Abelian decomposition tells that this is not true, and shows how to separate the colored chromons unambiguously.

Moreover, the Abelian decomposition decomposes the restricted potential (the binding gluons) further to the non-topological Maxwell part (the neurons) and topological Dirac part (the monopoles) gauge independently. This allows us to study the role of the monopole, and prove that it is the monopole which is responsible for the confinement gauge independently [24–27]. As importantly, it allows us to calculate the QCD effective action and demonstrate the monopole condensation [28–30].

But what is most important for our purpose is that it helps us to have a clear picture of glueballs with which we can identify them. This is because the chromons (being colored) play the role of the constituent gluons while the neurons (being color neutral) bind them, after the confinement sets in. So we can construct the glueballs with a finite number of chromons as the constituent. This generalizes the quark model to the quark and chromon model which provides a new picture of hadrons [20, 21, 31].

The quark model has been very successful. But our quark and chromon model has many advantages. It predicts new hadronic states, for example the hybrid hadrons made of chromons and quarks. Moreover, it provides a clear picture of glueballs and their mixing with the iso-singlet quarkonia and allows us to calculate the gluon (chromon) content of the mesons. Of course, the constituent gluon model can also do that, but this model does not tell the difference between the binding gluons and the constituent gluons.

To understand this consider the hydrogen atom in QED. Obviously we have photons as well as electron and proton in it, but only the electron and proton become the constituents because only they determine the atomic structure of the hydrogen atom in the periodic table. The photons play no role in the atomic structure. They are there as the electromagnetic field to provide the binding, not as the constituent of the atom.

Exactly the same way we have quarks and gluons in the proton. But again the gluons inside the proton do not play any role in the baryonic structure of the proton. This means that they must be the “binding” gluons, not the “constituent” gluons, which (just like the photons

in the hydrogen atom) provide only the binding of the quarks in the proton. If so, what are the constituent gluons, and how can we distinguish them from the binding gluons? Obviously the constituent model can not provide the answer.

The Abelian decomposition naturally resolves this difficulty. It tells that there are indeed two types of gluons, the binding gluons and the chromons, and in general only the chromons could be treated as the constituent gluons [20, 21]. This is because the binding gluons provide the binding force for colored objects, but the chromons (just like the quarks) become the colored source which make bound states in QCD. So (with few exceptions) only the chromons could be qualified to be the constituent of hadrons.

And the proton has no constituent chromons. But we emphasize that this does not mean protons do not contain the chromons at all. Clearly the three valence quarks which make up the proton can exchange chromons among themselves. Moreover, protons could have an infinite number of “the sea chromons”, just as they have the sea quarks. But obviously these chromons are not the constituent chromons.

In the quark and chromon model one could (in principle) construct an infinite number of glueballs with chromons. So one might ask why experimentally we have not so many candidates of them. There are two reasons why this is so. First, the glueballs made of chromons have an intrinsic instability [29, 30]. So they have broad widths, and this is in addition to the normal hadronic decay width. This means that they have a relatively short life-time. So only the low-lying glueballs could actually be observed experimentally. This is because the chromons, unlike the quarks, tend to annihilate each other in the chromo-electric background. This must be contrasted with quarks, which remain stable inside the hadrons.

This is closely related to the asymptotic freedom (anti-screening) of gluons. It is well known that in QED the strong electric background tends to generate the pair creation of electrons, which makes the charge screening [32–34]. But in QCD gluons and quarks play opposite roles in the asymptotic freedom. The quarks enhance the screening while the gluons diminish it to generate the anti-screening [35, 36]. In fact in the presence of a chromo-electric background the chromon loop generates a negative imaginary part but the quark loop generates a positive imaginary part in the QCD effective action. This tells that the chromo-electric field tends to generate the pair creation of the quarks but the pair annihilation of the chromons [29, 30, 37–39].

Second, in our model the glueballs inevitably mix with quarkonia, so that in general they do not appear as mass eigenstates. So, to identify the glueballs, we have to consider the possible mixing with the quarkonia. This makes the experimental identification of glueballs a nontrivial

matter. This is another reason why the experimental identification of the glueballs so far has not been so successful.

Of course, in rare cases we could have the pure glueballs called the oddballs [7, 31]. This is because some of the  $gg$  chromoballs have the quantum number  $J^{PC}$  which can not be made possible with  $q\bar{q}$ . In this case there is no  $q\bar{q}$  which could mix with the oddballs, so that they may exist as pure chromoballs. This makes the identification of the oddballs an important issue in QCD.

In a recent paper we have discussed the general framework of hadron spectroscopy based on the quark and chromon model, and showed how the model can explain the glueball-quarkonium mixing and allow us to identify the glueballs [31]. The present paper is the succession in which we extend the preceding work and discuss the numerical analysis of the glueball-quarkonium mixing in more detail to help identify the glueballs without much ambiguity.

Our analysis makes it clear that the chromoballs play the central role in the meson spectroscopy, although in general they do not appear as mass eigenstates. In particular, our analysis tells that the quarkonium-chromoball mixing makes a deep influence on the  $q\bar{q}$  octet-singlet mixing. In fact in the quark and chromon model the  $q\bar{q}$  octet-singlet mixing can not be discussed without the quarkonium-chromoball mixing, because the quarkonium-chromoball mixing inevitably induces the octet-singlet mixing.

The paper is organized as follows. In Section II we review the Abelian decomposition and the confinement mechanism for later purpose. In Section III we argue that in the quark and chromon model the chromoballs, the bound states of chromons, can be understood as the glueballs. But we also discuss the possibility that the neurons could form very loosely bound states. In Section IV we discuss the glueball-quarkonium mixing mechanism. In Section V we present the numerical analysis of the low-lying glueball-quarkonium mixing in  $0^{++}$ ,  $2^{++}$ , and  $0^{-+}$  sectors below 2 GeV, and show that  $f_0(500)$ ,  $f_0(1500)$ ,  $f_2(1950)$ ,  $\eta(1405)$ , and  $\eta(1475)$  become the strong candidates of glueballs. Finally in the last section we discuss the physical implications of our analysis.

## II. NEURONS AND CHROMONS: A REVIEW

It is well known that QCD can be understood as the extended QCD (ECD), namely RCD made of the binding gluons which has the valence gluons as colored source [20–22]. This follows from the Abelian decomposition of QCD which decomposes the gauge potential to the restricted part and the valence part gauge independently.

Consider the SU(3) QCD made of eight gluons,

$$\mathcal{L}_{QCD} = -\frac{1}{4}\vec{F}_{\mu\nu}^2. \quad (1)$$

To have the Abelian decomposition, let  $\hat{n}_i$  ( $i = 1, 2, \dots, 8$ ) be an arbitrary local orthonormal SU(3) basis. Now choose the Abelian directions to be  $\hat{n}_3 = \hat{n}$  and  $\hat{n}_8 = \hat{n}'$ , and make the Abelian projection by

$$D_\mu \hat{n} = 0. \quad (2)$$

This automatically guarantees [40]

$$D_\mu \hat{n}' = 0, \quad \hat{n}' = \frac{1}{\sqrt{3}} \hat{n} * \hat{n}. \quad (3)$$

where  $*$  denotes the  $d$ -product. This is because SU(3) has two vector products, the anti-symmetric  $f$ -product and the symmetric  $d$ -product.

Solving (2), we have the Abelian projection which projects out the binding potential,

$$\begin{aligned} \vec{A}_\mu &\rightarrow \hat{A}_\mu = A_\mu \hat{n} + A'_\mu \hat{n}' - \frac{1}{g} \hat{n} \times \partial_\mu \hat{n} - \frac{1}{g} \hat{n}' \times \partial_\mu \hat{n}' \\ &= \sum_p \frac{2}{3} \hat{A}_\mu^p, \quad (p = 1, 2, 3), \\ \hat{A}_\mu^p &= A_\mu^p \hat{n}^p - \frac{1}{g} \hat{n}^p \times \partial_\mu \hat{n}^p = \mathcal{A}_\mu^p + \mathcal{C}_\mu^p, \\ \mathcal{A}_\mu^p &= A_\mu^p \hat{n}^p, \quad \mathcal{C}_\mu^p = -\frac{1}{g} \hat{n}^p \times \partial_\mu \hat{n}^p, \\ A_\mu^1 &= A_\mu, \quad A_\mu^2 = -\frac{1}{2} A_\mu + \frac{\sqrt{3}}{2} A'_\mu, \\ A_\mu^3 &= -\frac{1}{2} A_\mu - \frac{\sqrt{3}}{2} A'_\mu, \quad \hat{n}^1 = \hat{n}, \\ \hat{n}^2 &= -\frac{1}{2} \hat{n} + \frac{\sqrt{3}}{2} \hat{n}', \quad \hat{n}^3 = -\frac{1}{2} \hat{n} - \frac{\sqrt{3}}{2} \hat{n}', \end{aligned} \quad (4)$$

where the sum is the sum of the Abelian directions of three SU(2) subgroups made of  $(\hat{n}_1, \hat{n}_2, \hat{n}^1)$ ,  $(\hat{n}_6, \hat{n}_7, \hat{n}^2)$ ,  $(\hat{n}_4, -\hat{n}_5, \hat{n}^3)$ . Notice that the three  $\hat{A}_\mu^p$  are not mutually independent.

From this we have the restricted field strength

$$\hat{F}_{\mu\nu} = \frac{2}{3} \sum_p \hat{F}_{\mu\nu}^p, \quad (5)$$

which is made of two binding gluons. With this we have the restricted QCD (RCD) [20–22]

$$\begin{aligned} \mathcal{L}_{RCD} &= -\frac{1}{4} \hat{F}_{\mu\nu}^2 = -\frac{1}{6} \sum_p (\hat{F}_{\mu\nu}^p)^2 \\ &= -\frac{1}{6} \sum_p (F_{\mu\nu}^p + H_{\mu\nu}^p)^2, \\ F_{\mu\nu}^p &= \partial_\mu A_\nu^p - \partial_\nu A_\mu^p, \\ H_{\mu\nu}^p &= -\frac{1}{g} \hat{n}^p \cdot (\partial_\mu \hat{n}^p \times \partial_\nu \hat{n}^p), \end{aligned} \quad (6)$$

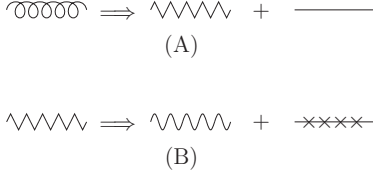


FIG. 1: The Abelian decomposition of the gluons. The gluon is decomposed to the binding gluon (kinked line) and the chromon (straight line) in (A), and the binding gluon is further decomposed to the neuron (wiggly line) and the monopole (spiked line) in (B).

which has the full SU(3) gauge symmetry. Notice that it has a dual structure, made of the electric potentials  $\mathcal{A}_\mu^p$  which describe the neurons and the magnetic potentials  $\mathcal{C}_\mu^p$  which describe the monopoles.

With (4) we have the Abelian decomposition of the SU(3) gauge potential,

$$\begin{aligned}\vec{A}_\mu &= \hat{A}_\mu + \vec{X}_\mu = \sum_p \left( \frac{2}{3} \hat{A}_\mu^p + \vec{W}_\mu^p \right), \\ \vec{X}_\mu &= \sum_p \vec{W}_\mu^p, \\ \vec{W}_\mu^1 &= X_\mu^1 \hat{n}_1 + X_\mu^2 \hat{n}_2, \quad \vec{W}_\mu^2 = X_\mu^6 \hat{n}_6 + X_\mu^7 \hat{n}_7, \\ \vec{W}_\mu^3 &= X_\mu^4 \hat{n}_4 - X_\mu^5 \hat{n}_5.\end{aligned}\quad (7)$$

Here the valence potential  $\vec{X}_\mu$  transforms gauge covariantly, and can be decomposed to the three valence gluons  $\vec{W}_\mu^p$  of the SU(2) subgroups. But unlike  $\hat{A}_\mu^p$ , they are mutually independent. So we have two binding gluons and six valence gluons (the chromons) in SU(3) QCD. The Abelian decomposition has also been known as the Cho decomposition, Cho-Duan-Ge decomposition, or Cho-Faddeev-Niemi decomposition [41–44].

The Abelian decomposition of the gluons given by (4) and (7) can be summarized graphically. This is shown in Fig. 1, where the gluons are decomposed to the binding gluons and the valence gluons in (A), and the binding gluons are decomposed further to the non-topological Maxwell part  $\mathcal{A}_\mu$  (the neurons) and the topological Dirac part  $\mathcal{C}_\mu$  (the monopoles) in (B).

From (7) we have

$$\begin{aligned}\hat{D}_\mu \vec{X}_\nu &= \sum_p \hat{D}_\mu^p \vec{W}_\nu^p, \quad \hat{D}_\mu^p = \partial_\mu + g \hat{A}_\mu^p \times, \\ \vec{X}_\mu \times \vec{X}_\nu &= \sum_{p,q} \vec{W}_\mu^p \times \vec{W}_\nu^q, \\ \vec{F}_{\mu\nu} &= \hat{F}_{\mu\nu} + \hat{D}_\mu \vec{X}_\nu - \hat{D}_\nu \vec{X}_\mu + g \vec{X}_\mu \times \vec{X}_\nu \\ &= \sum_p \left[ \frac{2}{3} \hat{F}_{\mu\nu}^p + (\hat{D}_\mu^p \vec{W}_\nu^p - \hat{D}_\nu^p \vec{W}_\mu^p) \right] \\ &\quad + \sum_{p,q} \vec{W}_\mu^p \times \vec{W}_\nu^q,\end{aligned}\quad (8)$$

so that we can express (1) to the following SU(3) ECD [28–30]

$$\mathcal{L}_{ECD} = \mathcal{L}_{RCD} - \frac{1}{4} (\hat{D}_\mu \vec{X}_\nu - \hat{D}_\nu \vec{X}_\mu)^2$$

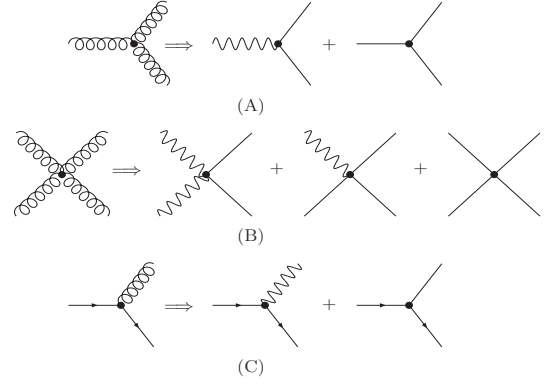


FIG. 2: The decomposition of vertices in SU(3) QCD. The three and four point gluon vertices are decomposed in (A) and (B), and the quark gluon vertices are decomposed in (C).

$$\begin{aligned}& -\frac{g}{2} (\hat{D}_\mu \vec{X}_\nu - \hat{D}_\nu \vec{X}_\mu) \cdot (\vec{X}_\mu \times \vec{X}_\nu) \\ & -\frac{g}{2} \hat{F}_{\mu\nu} \cdot (\vec{X}_\mu \times \vec{X}_\nu) - \frac{g^2}{4} (\vec{X}_\mu \times \vec{X}_\nu)^2 \\ & = \sum_p \left[ -\frac{1}{6} (\hat{F}_{\mu\nu}^p)^2 - \frac{1}{4} (\hat{D}_\mu^p \vec{W}_\nu^p - \hat{D}_\nu^p \vec{W}_\mu^p)^2 \right. \\ & \quad \left. - \frac{g}{2} \hat{F}_{\mu\nu}^p \cdot (\vec{W}_\mu^p \times \vec{W}_\nu^p) \right] \\ & \quad - \sum_{p,q} \frac{g^2}{4} (\vec{W}_\mu^p \times \vec{W}_\nu^q)^2 \\ & \quad - \sum_{p,q,r} \frac{g}{2} (\hat{D}_\mu^p \vec{W}_\nu^p - \hat{D}_\nu^p \vec{W}_\mu^p) \cdot (\vec{W}_\mu^q \times \vec{W}_\nu^r) \\ & \quad - \sum_{p \neq q} \frac{g^2}{4} [(\vec{W}_\mu^p \times \vec{W}_\nu^q) \cdot (\vec{W}_\mu^q \times \vec{W}_\nu^p) \\ & \quad + (\vec{W}_\mu^p \times \vec{W}_\nu^p) \cdot (\vec{W}_\mu^q \times \vec{W}_\nu^q)].\end{aligned}\quad (9)$$

This is the reconstruction of QCD by the Abelian decomposition, which is mathematically identical to the QCD Lagrangian (1). Adding an extra term or subtracting any existing term is strictly forbidden. But clearly in this expression QCD acquires a totally new meaning.

This shows that QCD is nothing but RCD which interacts with six colored chromons, which means that the chromons (just like the quarks) do not play an important role in the color confinement. This tells that RCD is essential for the confinement. Clearly the dual structure of RCD plays the crucial role in the monopole condensation and the confinement. On the other hand, after the monopole condensation RCD contains only the neurons. In this case RCD, just like the pure Maxwell's theory without electron in QED, becomes essentially a free theory where the two neurons interact only through the quark or chromon loops.

We can easily add quarks in the Abelian decomposition,

$$\begin{aligned}\mathcal{L}_q &= \sum_k \bar{\Psi}_k (i\gamma^\mu D_\mu - m) \Psi_k \\ &= \sum_k \left[ \bar{\Psi}_k (i\gamma^\mu \hat{D}_\mu - m) \Psi_k + \frac{g}{2} \vec{X}_\mu \cdot \bar{\Psi}_k (\gamma^\mu \vec{t}) \Psi_k \right]\end{aligned}$$

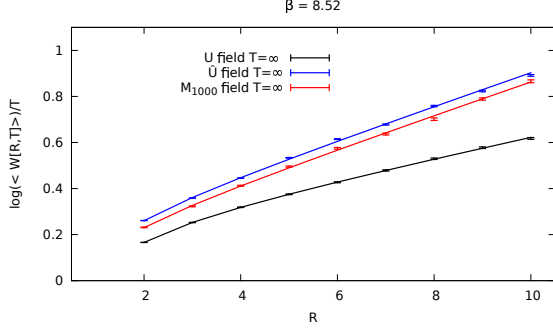


FIG. 3: The lattice QCD calculation which establishes the monopole dominance in Wilson loop. Here the black, red, and blue slopes are obtained with the full potential, the restricted potential, and the monopole potential, respectively.

$$= \sum_{p,k} \left[ \bar{\Psi}_k^p (i\gamma^\mu \hat{D}_\mu^p - m) \Psi_k^p + \frac{g}{2} \vec{W}_\mu^p \cdot \bar{\Psi}_k^p (\gamma^\mu \vec{\tau}^p) \Psi_k^p \right],$$

$$\hat{D}_\mu = \partial_\mu + \frac{g}{2i} \vec{t} \cdot \hat{A}_\mu, \quad \hat{D}_\mu^p = \partial_\mu + \frac{g}{2i} \vec{\tau}^p \cdot \hat{A}_\mu^p, \quad (10)$$

where  $m$  is the mass,  $k$  is the flavor index,  $\vec{t}$  is the color generators of the quark triplet corresponding to the chromons  $\vec{X}_\mu$ ,  $p$  denotes the color generators of the quarks corresponding to three SU(2) subgroups of SU(3), and  $\Psi_k^p$  represents the three SU(2) quark doublets (i.e., (r,b), (b,g), and (g,r) doublets) of the (r,b,g) quark triplet. With this the colors of the six chromons are given by  $(r\bar{b}, b\bar{g}, g\bar{r}, \bar{r}b, \bar{b}g, \bar{g}r)$ , which we express by  $(R, B, G, \bar{R}, \bar{B}, \bar{G})$ .

What is remarkable about (9) and (10) is that it is Weyl symmetric, symmetric under the permutation of the three SU(2) subgroups of SU(3). This is important, because this tells that after the Abelian decomposition the Weyl group (more precisely the color reflection group) becomes the residual symmetry which replaces the SU(3) symmetry and plays the role of the color gauge symmetry [20, 21].

As importantly, they show that we can decompose and clarify the Feynman diagrams in QCD. This is shown in Fig.2. In (A) the three-point QCD gluon vertex is decomposed to two vertices made of one neuron plus two chromons and three chromons. In (B) the four-point gluon vertex is decomposed to three vertices made of one neuron plus three chromons, two neurons plus two chromons, and four chromons. In (C) the quark-gluon vertex is decomposed to the quark-neuron vertex and quark-chromon vertex.

Notice that here three-point vertex made of three neurons or two neurons and one chromon, and four-point vertex made of three or four neurons are forbidden by the conservation of color. Moreover, the quark-neuron interaction does not change the quark color, but the quark-chromon interaction changes the quark color.

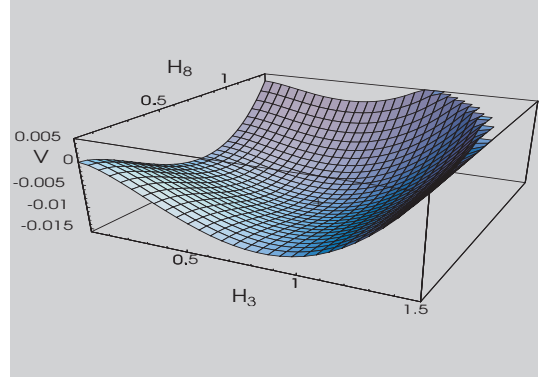


FIG. 4: The one-loop effective potential of SU(3) QCD which demonstrates the monopole condensation. The potential is obtained by integrating out the chromons in the presence of a constant monopole background.

Another point is that in these diagrams the monopoles do not appear. This is because, after the confinement (the monopole condensation) sets in, only the neurons remain in the binding gluons. So, in the perturbative regime (at the core of hadrons where the asymptotic freedom applies) only the neurons and chromons contribute to the Feynman diagrams.

Our analysis tells that, although the Abelian decomposition does not change QCD, it shows that the gauge potential can be decomposed to the non-topological neurons and chromons and the topological monopoles which play different roles. Perturbatively (in terms of the Feynman diagrams) the neurons play the role of the photon and the chromons play the role of (massless) charged vector fields in QED. And there is no place for the monopoles here. Non-perturbatively, however, the monopoles become the confining agents and the others become the confined prisoners. Without the Abelian decomposition we can not tell this difference because all gluons are treated on equal footing. This is the advantage of ECD over QCD.

This can be demonstrated. First, implementing the Abelian decomposition on lattice, we can calculate the contribution of the Wilson loop with the full potential, the restricted potential, and the monopole potential separately, and show that the monopole potential produces the confining force gauge independently [24–27]. The lattice result obtained by [26, 27] is copied in Fig. 3.

Second, with the Abelian decomposition we can calculate the QCD effective action in the presence of the monopole background and show that the true QCD vacuum is given by the monopole condensation, more precisely the monopole-antimonopole pair condensation [29, 30]. The effective potential obtained by [30] is copied in Fig. 4. This strongly implies that it is the monopole condensation which generates the mass gap and the confinement in QCD. Of course, similar results have been

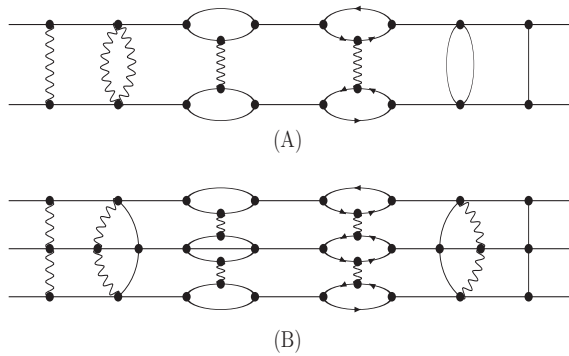


FIG. 5: The possible Feynman diagrams which bind the chromons. Two chromon binding is shown in (A), three chromon binding is shown in (B). The arrowed loops represent the quark loops.

obtained with QCD. But most of the calculations were gauge dependent, which have made the results unreliable.

There are other advantages. As we have already mentioned, ECD provides a new set of Feynman diagrams in which the neurons and chromons play different roles. But what is important for our purpose is the generalization of the quark model to the quark and chromon model which allows us to identify the glueballs more easily.

### III. CHROMOBALLS: GLUEBALLS IN QUARK AND CHROMON MODEL

In the preceding paper we have outlined how we can construct the glueballs with chromons [31]. The general picture of the glueballs in our model is very similar to the glueballs in the constituent gluon model, so that we can construct color singlet glueballs with  $gg$  or  $ggg$  [7, 8]. The difference, of course, is that in our case there are two types of gluons, and only the six chromons which carry the color charge could become the constituent gluons. This is because the other two gluons (the neurons) are color neutral. So our glueballs could actually be understood as the chromoballs.

To clarify this point we compare the possible Feynman diagrams of two and three chromon interactions shown in Fig. 5 with the similar Feynman diagrams of neuron interactions shown in Fig. 6. Clearly Fig. 5 looks very similar to the Feynman diagrams of  $q\bar{q}$  and  $qqq$  bound states in the quark model. This means that the colored chromons, just like the colored quarks, can become the constituents of hadrons. In particular, this means that they could form chromoball bound states among themselves.

On the other hand Fig. 6 looks totally different from Fig. 5. Obviously Fig. 6 looks very much like the photon self-interaction in QED. This is because the neurons are

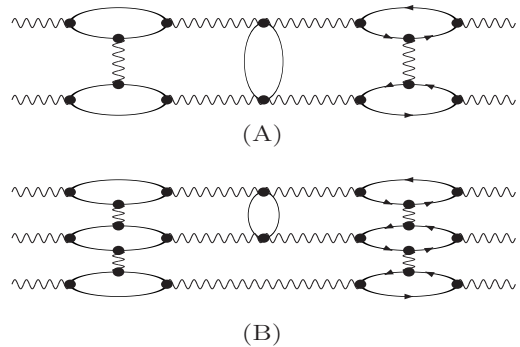


FIG. 6: The possible Feynman diagrams of the neuron interaction. Two neuron binding is shown in (A), three neuron binding is shown in (B). The quark loops are denoted by the arrows.

not colored, so that they can interact only through the chromon or quark loops. So they actually play the role of “the photons” in QCD whose binding is much weaker than the chromon binding.

The interesting question is whether the neuron binding is strong enough to form a bound state. Since the photons in QED do not form a bound state, we might suppose that the color neutral neurons do not form a bound state either. In this case the neurons do not qualify to be the constituent of hadrons.

This conclusion, however, may be premature and need clarification. Although Fig. 6 tells that the neuron interaction is similar to the photon self-interaction in QED, the QCD coupling is much stronger than the QED coupling. So, the fact that the photons do not form a bound state does not guarantee that the neurons do not make bound states. Moreover, Fig. 6 shows that the two neuron interaction actually looks very much like the interaction between two  $q\bar{q}$  mesons or two chromoball bound states, and there is no reason why two mesons can not form a bound state.

So, if the neurons form a bound state at all, they should form a very weakly bound state which would look much like a bound state of two quarkonia or a molecular state made of two light mesons. This means that there could be only a few neuroballs, the bound states made of neurons, maybe one or two if at all. This point will become very important in our numerical mixing analysis in the following.

Another point is the role of chromons in binding the colored source. Clearly Fig. 5 (and Fig. 6) show that the chromons (as well as the neurons) can exchange chromons and contribute to the binding. This shows that the colored objects could generate the binding force exchanging chromons. But there is a clear difference between the role of the chromon to be the constituent gluon and the exchange gluon. Independent of whether the chromons

contribute to the binding or not, what must be obvious is that the chromons can not escape from the role of the constituent gluons, simply because they are the colored source of QCD.

At this point one might wonder how the six chromons could form a color singlet. To understand this we have to keep in mind that the chromons and neurons are defined only after the Abelian decomposition, after we select the Abelian directions. But since changing the signature of the Abelian directions does not change the Abelian decomposition, the chromons and neurons are defined up to the residual symmetry called the color reflection invariance [21, 22, 31]. This means that after the Abelian decomposition the color gauge symmetry is reduced to the discrete symmetry given by the color reflection group, and the SU(3) color gauge invariance translates to the color reflection invariance.

This observation tells that the chromons are defined only up to the color reflection under which they change the color. In other words, the chromons should form a representation of the color reflection group, so that only the color reflection invariant combinations of the chromons become gauge invariant and thus form the glueballs.

Obviously the color reflection group should form a subgroup of the original gauge group, so that for SU(N) it has an  $N \times N$  matrix representation. For SU(2) it is made of 4 elements and for SU(3) it is made of 24 elements. The color reflection group has the Weyl group, the symmetry group of the root space of the original group, as a proper subgroup. The Weyl group of SU(N) is  $S_N$ , the symmetric group of degree  $N$  which is the permutation group of  $N$  elements. And the chromons form the regular representation of the Weyl group [45, 46].

We can obtain the Weyl group factorizing out the trivial subgroup made of the diagonal elements from the color reflection group. In SU(3) the three chromons ( $R, G, B$ ) and anti-chromons ( $\bar{R}, \bar{G}, \bar{B}$ ) form triplet representations, and the six chromons ( $R, G, B, \bar{R}, \bar{G}, \bar{B}$ ) form a sextet representation of the Weyl group [45, 46]. We present the SU(3) color reflection group and the Weyl group in the appendix.

As we have pointed out, the chromoballs have an intrinsic instability coming from the annihilation of chromons in the color background (the anti-screening of the color charge) [29–31, 37–39]. We can estimate the glueball partial decay width coming from this instability. According to the QCD one-loop effective action the chromon annihilation probability per unit volume per unit time is given by [29–31]

$$\Gamma_A = \sum_p \frac{11g^2}{96\pi} \bar{E}_p^2 \times \frac{4\pi}{3\Lambda_{QCD}^3}, \quad (11)$$

where the sum is on three SU(2) subgroups and  $\bar{E}_p$  is the average chromo-electric field of each subgroup inside the

glueballs. Now, if we choose  $\alpha_s \simeq 0.4$ ,  $\Lambda_{QCD} \simeq 339 \text{ MeV}$  (for three quark flavors), and  $\bar{E}_p \simeq (g/\pi)\Lambda_{QCD}^2$  we have  $\Gamma_A \simeq 398 \text{ MeV}$  [17]. But notice that with  $\Lambda_{QCD} \simeq 200 \text{ MeV}$ , we have  $\Gamma_A \simeq 235 \text{ MeV}$  [47].

Of course this is a rough estimate which depends on many things. For example, the  $gg$  glueballs and  $ggg$  glueballs may have different color field strengths and different sizes, and thus may have different life-time. But we emphasize that the above estimate is the partial decay width we expect from the asymptotic freedom, in addition to the “normal” hadronic decay width. This strongly implies that in general the glueballs (in particular excited ones) are expected to have very short lifetime, and become difficult to be observed. This could be another reason why it is not easy to identify the glueball states experimentally.

This instability has another important implication. It has been widely believed that “the gluon condensation” plays important role in QCD dynamics [6]. However, the gluon pair annihilation shown in (11) strongly suggests that this gluon condensation should become unstable, and thus can not last. Moreover, QCD already has the monopole condensation. This makes the gluon condensation highly improbable.

In the quark and chromon model it is natural to expect that the chromons (just like the quarks) acquire a constituent mass after the confinement sets in. So we may assume that in general the  $ggg$  glueballs are heavier than the  $gg$  glueballs. As we will see, the constituent chromon mass plays an important role in the mixing analysis.

#### IV. GLUEBALL-QUARKONIUM MIXING

Now we are ready to discuss the glueball-quarkonium mixing. The possible Feynman diagrams for the mixing are shown in Fig. 7, which tells that the mixing takes place not just between quarkonia and chromoballs but also between the  $gg$  and  $ggg$  chromoballs, directly or through the virtual states made of neurons.

Obviously the mixing influences the  $q\bar{q}$  octet-singlet mixing in the quark model. So we review the octet-singlet mixing in the quark model first. Let

$$\begin{aligned} \langle u\bar{u}|H|u\bar{u}\rangle_{Ex} &= \langle d\bar{d}|H|d\bar{d}\rangle_{Ex} = E, \\ \langle s\bar{s}|H|s\bar{s}\rangle_{Ex} &= E' = E + \Delta, \\ \langle q'\bar{q}'|H|q\bar{q}\rangle_{An} &= A, \quad (\text{for all } q, q'). \end{aligned} \quad (12)$$

Now with

$$\begin{aligned} |8\rangle &= \frac{|u\bar{u}\rangle + |d\bar{d}\rangle - 2|s\bar{s}\rangle}{\sqrt{6}}, \\ |1\rangle &= \frac{|u\bar{u}\rangle + |d\bar{d}\rangle + |s\bar{s}\rangle}{\sqrt{3}}, \end{aligned} \quad (13)$$



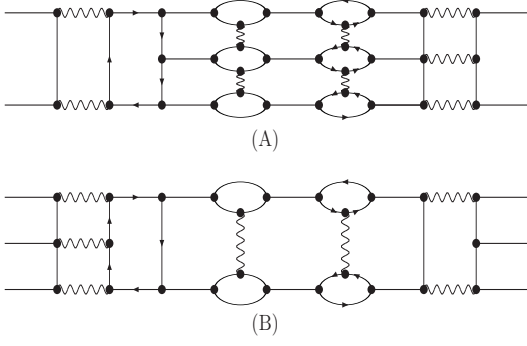


FIG. 7: The possible glueball-quarkonium mixing diagrams. The  $gg$  and  $ggg$  mixing with quarkonia are shown in (A) and (B).

we may obtain the following mass matrix for the  $q\bar{q}$  which describes the octet-singlet mixing,

$$M^2 = \begin{pmatrix} \langle 8|H|8 \rangle & \langle 8|H|1 \rangle \\ \langle 1|H|8 \rangle & \langle 1|H|1 \rangle \end{pmatrix} = \begin{pmatrix} E + \frac{2}{3}\Delta & -\frac{\sqrt{2}}{3}\Delta \\ -\frac{\sqrt{2}}{3}\Delta & E + \frac{1}{3}\Delta + 3A \end{pmatrix}. \quad (14)$$

Notice that  $\Delta$ -term is responsible for the mixing. But we emphasize that this mixing among the quarks can not provide the correct octet-singlet mixing because the glueballs inevitably influence the quark octet-singlet mixing. This is evident in Fig. 7.

Of course, we could also have similar diagrams in QCD. If so, one might ask what is the difference between the quark model and the quark and chromon model. An obvious difference is that we have two types of gluons in Fig. 7. This has deep implications. To see this, let us compare our model with the “model independent” QCD sum rule approach which use the gauge invariant current operator to calculate the glueball mass [6]. As an example, consider the gauge invariant  $0^{++}$  current operator with which one can calculate the mass of the scalar glueball. In QCD the simplest such operator is given by  $\langle \vec{F}_{\mu\nu} \cdot \vec{F}_{\mu\nu} \rangle$  which supposedly describes the glueball made of two gluons. Similarly, for the  $2^{++}$  current operator we have  $\langle \vec{F}_{\mu\alpha} \cdot \vec{F}_{\alpha\nu} \rangle$ . But actually these operators contain two, three, and four gluon states, so that it is difficult to justify them as two gluon states.

On the other hand in our model the simplest  $0^{++}$  and  $2^{++}$  operators are just two chromon states given by  $\langle \vec{X}_\mu \cdot \vec{X}_\mu \rangle$  and  $\langle \vec{X}_\mu \cdot \vec{X}_\nu \rangle$  [20–22]. Similarly, for the glueballs made of three chromons we have  $\langle d_{abc} X_\mu^a X_\nu^b X_\rho^c \rangle$  and  $\langle f_{abc} X_\mu^a X_\nu^b X_\rho^c \rangle$ . This is simply impossible in the conventional QCD. This is the advantage of the Abelian decomposition.

Clearly we can calculate the chromoball mass with the above two chromon and three chromon operators. But before doing this we have to check if our model can explain the glueball-quarkonium mixing well. To do this consider the following  $3 \times 3$  mixing mass matrix of one lightest  $gg$  chromoball  $|G\rangle$  with the quark nonet [31]

$$M^2 = \begin{pmatrix} E + \frac{2}{3}\Delta & -\frac{\sqrt{2}}{3}\Delta & 0 \\ -\frac{\sqrt{2}}{3}\Delta & E + \frac{1}{3}\Delta + 3A & \nu \\ 0 & \nu & G \end{pmatrix}. \quad (15)$$

Of course similar mixing matrix has been used in the constituent gluon model. As we have pointed out, however, this model has a critical defect. And our quark and chromon model can be viewed as a new model which justifies the above mixing without such defect.

In principle we should be able to calculate the parameters in the mass matrix. For example, we could calculate  $G$  using the gauge invariant current operator discussed above, and calculate the mixing parameter  $\nu$  using the Feynman diagrams in our model. But here we will fix the parameters with experimental data to see how well the mixing matrix can explain the glueball-quarkonium mixing.

Now, diagonalizing the mass matrix we can transform the unphysical states ( $|8\rangle, |1\rangle, |G\rangle$ ) to the mass eigenstates ( $|m_1\rangle, |m_2\rangle, |m_3\rangle$ ), and obtain the information on the chromon and quark contents of the physical states. Notice that, assuming that after the confinement the chromons acquire the constituent mass  $\mu$ , we can put  $G = 4\mu^2$  (supposing the chromoball mass before the mixing is given by  $\sqrt{G} = 2\mu$ ).

We can easily generalize the mass matrix to the  $4 \times 4$  mixing

$$M^2 = \begin{pmatrix} E + \frac{2}{3}\Delta & -\frac{\sqrt{2}}{3}\Delta & 0 & 0 \\ -\frac{\sqrt{2}}{3}\Delta & E + \frac{1}{3}\Delta + 3A & \nu & \nu' \\ 0 & \nu & G & \epsilon \\ 0 & \nu' & \epsilon & G' \end{pmatrix}, \quad (16)$$

to include one more  $gg$  or  $ggg$  chromoball state  $|G'\rangle$ . This has eight parameters, but we may reduce the parameters to seven by diagonalizing the  $2 \times 2$  chromoball mass matrix first and putting  $\epsilon = 0$ . With this we can express  $G$  and  $G'$  by the chromon mass  $\mu$  and put  $G = 4\mu^2$  and  $G' = 4\mu^2 + \delta$  for  $gg$  or  $G' = 9\mu^2 + \delta$  for  $ggg$ .

Clearly (15) and (16) demonstrate that the quarkonium-chromoball mixing inevitably influences the octet-singlet mixing of the quarkonia. This means that we can not discuss the  $q\bar{q}$  spectroscopy without the chromoballs.

Diagonalizing the mass matrix we can figure out the quark and chromon contents of the mass eigenstates.



Moreover, knowing the chromon content of the physical states, we can calculate the relative branching ratios of iso-singlet mesons made of heavy quarks, e. g., the  $J/\psi$  radiative decay to the physical states in each channel. This is because these decays are the Okubo-Zweig-Iizuka (OZI) suppressed process which can only be made possible through the intermediate chromoball states.

Let  $\alpha_i$  be the parameters of the mixing matrix which determine the gluon content of physical states  $|m_i\rangle$ . We can predict the relative branching ratios of  $J/\psi$  to  $\gamma X$  decays among the physical states with  $\alpha_i$ , because these decays are induced by the chromons. So, for the S wave decay (i.e., for  $0^{++}$  and  $2^{++}$ ) we have [31]

$$R\left(\frac{J/\psi \rightarrow \gamma X_k}{J/\psi \rightarrow \gamma X_i}\right) = \left(\frac{\alpha_k}{\alpha_i}\right)^2 \left(\frac{m_\psi^2 - m_k^2}{m_\psi^2 - m_i^2}\right)^3, \quad (17)$$

but for the P wave decay (i.e., for  $0^{-+}$ ) we expect to have

$$R\left(\frac{J/\psi \rightarrow \gamma X_k}{J/\psi \rightarrow \gamma X_i}\right) = \left(\frac{\alpha_k}{\alpha_i}\right)^2 \left(\frac{m_\psi^2 - m_k^2}{m_\psi^2 - m_i^2}\right)^5, \quad (18)$$

where the last term is the kinematic phase space factor. Clearly this argument can also be applied to similar OZI suppressed decays of heavy  $t\bar{t}$  or  $b\bar{b}$  iso-singlet mesons.

It must be pointed out that, although the chromoballs in general mix with the quarkoniums, in particular cases the pure chromoballs could exist. This is because some of the  $gg$  chromoballs become the oddballs which have the quantum number  $J^{PC}$  that  $q\bar{q}$  can not have, and thus can not mix with the quarkonia [7, 31]. Obviously these low-lying oddballs become very important for us to search for the pure chromoballs.

Independent of the details, however, we emphasize the clarity of the mixing mechanism in our quark and chromon model. All terms in the mass matrix have clear physical meaning. For example we can draw the Feynman diagram which represents the parameter  $\nu$  in (15), and could in principle calculate it theoretically.

## V. NUMERICAL ANALYSIS

The above discussion shows that the mixing analysis is a crucial step for us to identify the glueballs. For the  $3 \times 3$  mixing the mass matrix has five parameters, but we can fix  $E$  and  $\Delta$  from the  $q\bar{q}$  flavor octet data. So we need three inputs to fix the mass matrix completely. There are different ways to fix them. One way is to choose two mass eigenstates from PDG and treat  $G$  (or equivalently the chromon mass  $\mu$ ) as a free parameter, and find the best fit for  $\mu$  which could predict the third physical state and explain the PDG data best. Another way is to use all three mass eigenstates as the input, and determine the the chromon mass as well.

For the  $4 \times 4$  mixing the matrix has seven parameters, but we can reduce this number to five fixing two of them from the  $q\bar{q}$  flavor octet data. With this we may choose four mass eigenstates as the input (when available) and find the physical contents of the mass eigenstates, treating the chromon mass as the free parameters. Or we may choose three mass eigenstates as the input and predict the mass of the fourth physical state, imposing an extra constraint, e.g.,  $\nu' = \nu$  etc.

In the preceding paper we have discussed the numerical analysis of the mixing below 2 GeV in  $0^{++}$ ,  $2^{++}$  and  $0^{-+}$  channels with this strategy [31]. But the numerical analysis was preliminary and inconclusive, partly because it depends very much on how to choose the inputs. In the following we discuss the mixing in more detail, and improve the results of the preceding paper.

### A. $0^{++}$ channel

In this channel PDG lists five iso-singlet mesons,  $f_0(500)$ ,  $f_0(980)$ ,  $f_0(1370)$ ,  $f_0(1500)$ , and  $f_0(1710)$  below 2 GeV [17]. But the interpretation of the scalar mesons has been difficult and controversial, because some of them have unusually large decay width and some of them could be viewed as non- $q\bar{q}$  multi-quark states [12–14]. In this paper we try to figure out their physical content within the quark and chromon model with the following two important issues in mind.

The first issue is what should we choose to be the isotriplet partner of the flavor octet in this channel. This is very important because this determines the inputs  $E$  and  $\Delta$  in the mixing analysis. PDG suggests that the flavor octet partner of the  $0^{++}$  isosinglet are  $a_0(1450)$  and  $K_0^*(1430)$ , not  $a_0(980)$  and  $K_0^*(1430)$  [17]. Intuitively, this looks somewhat strange because this implies that the  $u$  and  $d$  quarks are heavier (or at least not lighter) than the  $s$  quark. So it is worth for us to study the possibility that  $a_0(980)$  and  $K_0^*(1430)$  become the octet partners.

The second issue is  $f_0(500)$  which has an unusually broad decay width. According to PDG it does not fit to the quark model well, and there have been suggestions that it could be either a tetra-quark state or a mixed state [48–54]. But there are other logical possibilities.

First, it could be viewed as a neuroball, the glueball made of neurons [31]. As we pointed out, the neurons (just like the photons in QED) have very weak binding because they can interact only through the quark or chromon loops. Nevertheless they could form a loosely bound state which has a broad decay width. And this is exactly what we find in  $f_0(500)$ . This is in line with the popular interpretation that  $f_0(500)$  is a tetra-quark state [48–54]. This is evident in Fig. (6), where the loops can be viewed as  $q\bar{q}$  or  $gg$  bound states.

Another possibility is that  $f_0(500)$  could be the monoball, the vacuum fluctuation mode of the monopole condensation, in QCD [31]. As we have pointed out, if the color confinement comes from the monopole condensation, QCD could have a  $0^{++}$  vacuum fluctuation mode [20, 21]. In this case  $f_0(500)$  becomes a natural candidate of this vacuum fluctuation. This suggests that  $f_0(500)$  may not be a simple chromoball or  $q\bar{q}$  state.

With this in mind, we can discuss the mixing. If we adopt the PDG view and identify  $a_0(1450)$  to be the isotriplet partner, we may choose [17]

$$\begin{aligned} E &= m^2(a_0), \quad a_0 = a_0(1450), \\ \Delta &= 2(m^2(K) - m^2(a_0)), \quad K = K_0^*(1430). \end{aligned} \quad (19)$$

as the input. But as we have remarked, it is worth for us to check whether this PDG view is correct or not. Since the strange meson of the flavor octet of this channel is  $K_0^*(1430)$ , one would expect the mass of the non-strange isotriplet partner to be less than 1430 MeV. In this case  $a_0(980)$  becomes a natural candidate of the isotriplet partner of the flavor octet, and we may choose

$$\begin{aligned} E &= m^2(a_0), \quad a_0 = a_0(980), \\ \Delta &= 2(m^2(K) - m^2(a_0)), \quad K = K_0^*(1430). \end{aligned} \quad (20)$$

as the input. So we have two possible inputs, (19) and (20).

In the preceding paper we have discussed the  $3 \times 3$  mixing with  $f_0(1500)$  and  $f_0(1710)$  as the input, adopting the PDG view (19) [31]. The result is copied in Table I. Notice that the table shown in the preceding paper had a typological mistake that the numbers in the last two columns (i.e.,  $R(m_2/m_1)$  and  $R(m_3/m_1)$ ) were interchanged. The table shown in this paper corrects this mistake.

The table shows that the third state (with mass around 1400 MeV) could be identified to be  $f_0(1370)$ , which becomes predominantly an  $s\bar{s}$  state. But the physical contents of two other states depend very much on the value of the chromon mass  $\mu$ . When  $\mu$  is around 760 MeV,  $f_0(1500)$  become predominantly a chromoball state and  $f_0(1710)$  becomes predominantly the  $u\bar{u} + d\bar{d}$  state.

On the other hand, when the chromon mass increases to 860 MeV,  $f_0(1500)$  becomes a  $u\bar{u} + d\bar{d}$  state and  $f_0(1710)$  quickly becomes a chromoball state. But  $f_0(1370)$  remains to be the  $s\bar{s}$  state, so that here the  $s\bar{s}$  state becomes lighter than the  $u\bar{u} + d\bar{d}$  state. This, of course, is due to the input (19). This is against the PDG interpretation, which suggests that  $f_0(1370)$  is the  $u\bar{u} + d\bar{d}$  state and  $f_0(1710)$  is the  $s\bar{s}$  state.

On the other hand if we adopt (20) as the input, we obtain Table II. Here we have chosen  $f_0(980)$  and  $f_0(1500)$  as the input. The result shows that when  $\mu \simeq 750$  MeV, the third state has mass around 1800 MeV and could be identified as  $f_0(1710)$ . In this case  $f_0(1500)$

remains predominantly a chromoball state, but  $f_0(1710)$  becomes predominantly the  $s\bar{s}$  state and  $f_0(980)$  becomes predominantly the  $u\bar{u} + d\bar{d}$  state. This of course is what we have expected from (20).

Clearly the two tables give different descriptions, and we have to know which is closer to the truth. One way to find which is better is to compare the predictions of the relative radiative decay ratios of  $J/\psi$  with the experimental data. Experimentally PDG has new data on the radiative decay of  $J/\psi$  to  $0^{++}$  states [17],

$$J/\psi \rightarrow \gamma f_0(1710) \rightarrow \begin{cases} \gamma K \bar{K} \simeq (8.5 + 1.2 - 0.9) \\ \times 10^{-4}, \\ \gamma \pi \pi \simeq (4.0 \pm 1.0) \times 10^{-4}, \\ \gamma \omega \omega \simeq (3.1 \pm 1.0) \times 10^{-4}, \\ \gamma \eta \eta \simeq (2.4 + 1.2 - 0.7) \\ \times 10^{-4}, \end{cases}$$

and

$$J/\psi \rightarrow \gamma f_0(1500) \rightarrow \begin{cases} \gamma \pi \pi \simeq (1.01 \pm 0.32) \times 10^{-4}, \\ \gamma \eta \eta \simeq (1.7 + 0.6 - 1.4) \\ \times 10^{-5}. \end{cases}$$

Of course this may not be the final data, because other decay modes could be discovered later. But assuming that this is the final result, we have

$$R(f_0(1710)/f_0(1500)) \simeq 15.3. \quad (21)$$

This is a very important piece of information, because this determines the glue content of the mass eigenstates.

Now, Table II predicts the relative radiative decay ratio to be  $R(f_0(1710)/f_0(1500)) \simeq 0.04$  (at  $\mu = 750$  MeV). Clearly this is not in line with (21), which is troublesome. In comparison, according to Table I we have  $R(f_0(1710)/f_0(1500)) \simeq 15.3$  (at  $\mu \simeq 856$  MeV). This is in good agreement with the PDG data, which implies that Table I is better. This in turn implies that  $a_0(1450)$ , not  $a_0(980)$ , could be the isotriplet partner of these isosinglet states. But this conclusion is premature because the contents of physical states in Table I is controversial and  $R(m_2/m_1)$  becomes very sensitive to the change of  $\mu$ .

Independent of whether this result is correct or not, however, the above  $3 \times 3$  mixing has a critical shortcoming in that it can explain the mixing of only three physical states, while here we have at least four physical states (excluding  $f_0(500)$ ) below 2 GeV. This strongly motivates us to go to the  $4 \times 4$  mixing. And this is independent of which input, (19) or (20), we choose.

So we consider the  $4 \times 4$  mixing (16) with two chromoball states  $^1S_0$  and  $^5D_0$  made of two chromons  $|G\rangle$  and  $|G'\rangle$ . Diagonalizing the two chromoball mass matrix first, we may put

$$\epsilon = 0, \quad G = 4\mu^2, \quad G' = G + \delta, \quad (22)$$

TABLE I: The numerical analysis of the  $3 \times 3$  mixing in the  $0^{++}$  channel, with  $a_0(1450)$ ,  $f_0(1500)$ , and  $f_0(1710)$  as the input. Here the third physical state can be identified as  $f_0(1370)$ .

$\mu$	$A$	$\nu$	$m_3$	$m_1 = f_0(1500)$			$m_2 = f_0(1710)$			$m_3$			$R(m_2/m_1)$	$R(m_3/m_1)$
				$u+d$	$s$	$G$	$u+d$	$s$	$G$	$u+d$	$s$	$G$		
0.76	0.27	0.18	1.40	0.07	0.00	0.93	0.73	0.20	0.07	0.19	0.80	0.00	0.05	0.00
0.78	0.23	0.31	1.40	0.26	0.01	0.73	0.59	0.16	0.25	0.15	0.83	0.02	0.14	0.02
0.80	0.18	0.36	1.39	0.44	0.01	0.54	0.45	0.12	0.43	0.11	0.87	0.02	0.59	0.05
0.82	0.14	0.35	1.39	0.62	0.02	0.36	0.30	0.08	0.62	0.09	0.90	0.01	1.26	0.07
0.84	0.09	0.29	1.39	0.79	0.02	0.18	0.15	0.04	0.80	0.05	0.93	0.01	3.26	0.09
0.86	0.04	0.07	1.39	0.96	0.03	0.01	0.01	0.00	0.99	0.03	0.97	0.00	85.71	0.12

TABLE II: The numerical analysis of the  $3 \times 3$  mixing in the  $0^{++}$  channel, with  $a_0 = a_0(980)$ ,  $f_0(980)$ , and  $f_0(1500)$  as the input. Here the third physical state could be identified as  $f_0(1710)$ .

$\mu$	$A$	$\nu$	$m_3$	$m_1 = f_0(980)$			$m_2 = f_0(1500)$			$m_3$			$R(m_2/m_1)$	$R(m_3/m_1)$
				$u+d$	$s$	$G$	$u+d$	$s$	$G$	$u+d$	$s$	$G$		
0.55	2.44	1.29	3.06	0.05	0.00	0.95	0.44	0.54	0.02	0.51	0.46	0.02	0.01	0.00
0.60	1.91	1.62	2.83	0.11	0.00	0.89	0.43	0.52	0.05	0.46	0.48	0.06	0.04	0.00
0.65	1.33	1.68	2.55	0.21	0.00	0.79	0.40	0.49	0.11	0.39	0.51	0.10	0.09	0.01
0.70	0.71	1.44	2.21	0.41	0.00	0.59	0.34	0.42	0.24	0.24	0.58	0.17	0.26	0.05
0.75	0.04	0.36	1.79	0.95	0.00	0.05	0.05	0.06	0.89	0.00	0.94	0.05	10.75	0.43

and consider the mixing of the two  $q\bar{q}$  states with two chromoballs which have mass  $\sqrt{G}$  and  $\sqrt{G'}$ . This has seven parameters, but we can fix two with (19) or (20) and four with the four mass eigenstates  $f_0(980)$ ,  $f_0(1370)$ ,  $f_0(1500)$ , and  $f_0(1710)$  as the input. With this we can diagonalize the mass matrix and find the physical contents of the mass eigenstates, treating the chromon mass  $\mu$  as the free parameter.

Now, adopting the PDG view (19) we obtain Table III, but with (20) we obtain Table IV. But the mathematical equations which we need to solve to diagonalize the mass matrix are very rigid which often have no solution, and this forces us to change the input data slightly to find the solutions. So here we have changed the four mass eigenstates to 990, 1400, 1505, and 1722 MeVs to obtain Table III, and to 990, 1370, 1505, 1800 MeVs to obtain Table IV.

The numerical result of Table III obtained with (19) suggests that  $f_0(980)$  is predominantly the  $^1S_0$  chromoball state and  $f_0(1370)$  is predominantly the  $s\bar{s}$  state. But  $f_0(1500)$  becomes largely the  $^5D_0$  chromoball state and  $f_0(1710)$  becomes largely the  $u\bar{u} + d\bar{d}$  state, although they have considerable mixing as the chromon mass increases to 600 MeV. This is in line with Table I. But here the  $u\bar{u} + d\bar{d}$  state remains heavier than the  $s\bar{s}$  state, which again is due to the input (19).

On the other hand, Table IV obtained with (20) tells

that  $f_0(980)$  and  $f_0(1710)$  are the  $u\bar{u} + d\bar{d}$  and  $s\bar{s}$  states, respectively. And  $f_0(1370)$  and  $f_0(1500)$  become the  $^1S_0$  and  $^5D_0$  chromoball states. Again this is consistent with Table II.

As for the  $J/\psi$  radiative decay branching ratio, Table III shows that  $R(f_0(1710)/f_0(1500)) \simeq 0.8$  when  $\mu = 0.60$ , and Table IV gives around 0.05 when  $\mu = 680$  MeV. Clearly both are too small compared to (21), so that we can not tell which is the isotriplet partner of the  $0^{++}$  isosinglet state.

The contrast between Table III and Table IV is unmistakable. This, of course, originates from the inputs (19) and (20). This analysis has both positive and negative sides. The positive side is that the result of the  $4 \times 4$  mixing, in particular the physical contents of the mass eigenstates, is consistent with the  $3 \times 3$  mixing analysis. But the disappointing point is that the  $4 \times 4$  analysis can not tell whether the PDG view that  $a_0(1450)$ , not  $a_0(980)$ , is the isotriplet partner of the  $0^{++}$  isosinglet state.

At this point one might wonder why we did not include  $f_0(500)$  in the mixing. The reason is that  $f_0(500)$  could be an extraordinary state which does not fit well to a  $q\bar{q}$  state, which often has been interpreted as a tetraquark state [48–54]. In our quark and chromon model there are two possible explanations for this.

TABLE III: The numerical analysis of the  $4 \times 4$  mixing in the  $0^{++}$  channel, with  $f_0(980)$ ,  $f_0(1370)$ ,  $f_0(1500)$ , and  $f_0(1710)$  as the input. Here  $a_0(1450)$  is identified as the isotriplet partner.

$\mu$	$m_1 = f_0(980)$				$m_2 = f_0(1370)$				$m_3 = f_0(1500)$				$m_4 = f_0(1710)$			
	$u+d$	$s$	$G$	$G'$	$u+d$	$s$	$G$	$G'$	$u+d$	$s$	$G$	$G'$	$u+d$	$s$	$G$	$G'$
0.50	0.01	0.01	0.99	0.00	0.19	0.81	0.00	0.01	0.13	0.00	0.00	0.86	0.68	0.18	0.01	0.13
0.52	0.03	0.03	0.94	0.00	0.18	0.80	0.01	0.01	0.17	0.01	0.02	0.81	0.62	0.17	0.04	0.17
0.54	0.06	0.05	0.88	0.01	0.18	0.79	0.01	0.01	0.21	0.01	0.04	0.74	0.55	0.15	0.06	0.24
0.56	0.09	0.08	0.82	0.01	0.18	0.79	0.02	0.01	0.26	0.01	0.08	0.65	0.47	0.13	0.08	0.33
0.58	0.13	0.11	0.75	0.01	0.18	0.78	0.03	0.01	0.32	0.01	0.14	0.53	0.38	0.10	0.08	0.44
0.60	0.17	0.14	0.67	0.02	0.17	0.77	0.05	0.01	0.38	0.01	0.22	0.39	0.27	0.07	0.07	0.58

$\mu$	$R(m_2/m_1)$	$R(m_3/m_1)$	$R(m_4/m_1)$	A	$\nu$	$\nu'$	$\delta$
0.50	0.01	0.54	0.06	0.25	0.19	0.24	1.35
0.52	0.01	0.54	0.10	0.21	0.41	0.28	1.30
0.54	0.02	0.54	0.16	0.17	0.53	0.32	1.26
0.56	0.03	0.54	0.22	0.13	0.61	0.36	1.22
0.58	0.04	0.54	0.31	0.07	0.66	0.40	1.20
0.60	0.06	0.54	0.43	0.01	0.68	0.42	1.21

TABLE IV: The numerical analysis of the  $4 \times 4$  mixing in the  $0^{++}$  channel, with  $f_0(980)$ ,  $f_0(1370)$ ,  $f_0(1500)$ , and  $f_0(1710)$  as the input. Here  $a_0(980)$  is identified as the isotriplet partner.

$\mu$	$m_1 = f_0(980)$				$m_2 = f_0(1370)$				$m_3 = f_0(1500)$				$m_4 = f_0(1710)$			
	$u+d$	$s$	$G$	$G'$	$u+d$	$s$	$G$	$G'$	$u+d$	$s$	$G$	$G'$	$u+d$	$s$	$G$	$G'$
0.67	0.86	0.00	0.14	0.01	0.13	0.04	0.83	0.04	0.01	0.01	0.00	0.98	0.01	0.96	0.03	0.01
0.68	0.90	0.00	0.05	0.05	0.04	0.01	0.94	0.01	0.05	0.06	0.00	0.89	0.01	0.93	0.01	0.05

$\mu$	$R(m_2/m_1)$	$R(m_3/m_1)$	$R(m_4/m_1)$	A	$\nu$	$\nu'$	$\delta$
0.67	4.17	4.21	0.11	0.08	0.40	0.13	0.47
0.68	7.07	5.73	0.26	0.07	0.25	0.35	0.40

First, as we have already pointed out, the monopole condensation responsible for the color confinement in QCD will most likely generate a  $0^{++}$  vacuum fluctuation mode [20, 21, 31]. In this case  $f_0(500)$ , with the broad decay width, becomes a natural candidate of the vacuum fluctuation.

Second, in our quark and chromon model  $f_0(500)$  could be interpreted as the neuroball, a loosely bound state of neurons [31]. As we have argued, Fig. 6 clearly tells that a neuron bound state might look very much like a molecular state made of two mesons. And this interpretation is consistent with the popular view that it is a tetra-quark state.

Nevertheless, there is no reason why  $f_0(500)$  can not mix with quarkonia and chromoballs. Actually, even when  $f_0(500)$  appears as a neuroball it makes sense to include it in the mixing, because the neuroball could be viewed as a glueball. This must be clear from Fig. 6

and Fig. 7. Moreover, even when  $f_0(500)$  becomes the monoball, the vacuum fluctuation of the monopole condensation, it could in principle mix with quarkonia and chromoballs. This justifies the  $5 \times 5$  mixing.

For this reason we consider the following  $5 \times 5$  mixing with two  $q\bar{q}$  and three glueballs which has nine parameters,

$$M^2 = \begin{pmatrix} E + \frac{2}{3}\Delta & -\frac{\sqrt{2}}{3}\Delta & 0 & 0 & 0 \\ -\frac{\sqrt{2}}{3}\Delta & E + \frac{1}{3}\Delta + 3A & \nu_0 & \nu_1 & \nu_2 \\ 0 & \nu_0 & G_0 & 0 & 0 \\ 0 & \nu_1 & 0 & G_1 & 0 \\ 0 & \nu_2 & 0 & 0 & G_2 \end{pmatrix}, \quad (23)$$

Here  $G_1$  and  $G_2$  are the  $^1S_0$  and  $^5D_0$  chromoball as before, but  $G_0$  is supposed to be the monoball or the neuroball. In this case we can put all five physical states

TABLE V: The numerical analysis of the  $5 \times 5$  mixing in the  $0^{++}$  channel, with all 5 mass eigenstates ( $f_0(500)$ ,  $f_0(980)$ ,  $f_0(1370)$ ,  $f_0(1500)$ , and  $f_0(1710)$ ) as the input. Here  $a_0(1450)$  is identified as the isotriplet partner.

$\mu_0$	$\mu$	$m_1 = f_0(500)$						$m_2 = f_0(980)$					$m_3 = f_0(1370)$					$m_4 = f_0(1500)$				
		$u + d$	$s$	$G_0$	$G_1$	$G_2$		$u + d$	$s$	$G_0$	$G_1$	$G_2$	$u + d$	$s$	$G_0$	$G_1$	$G_2$	$u + d$	$s$	$G_0$	$G_1$	$G_2$
0.28	0.50	0.00	0.00	1.00	0.00	0.00		0.00	0.00	0.00	1.00	0.00	0.18	0.81	0.00	0.00	0.01	0.13	0.00	0.00	0.00	0.87
0.30	0.52	0.01	0.01	0.97	0.00	0.00		0.03	0.02	0.01	0.94	0.00	0.18	0.80	0.00	0.01	0.01	0.18	0.01	0.01	0.02	0.79
0.32	0.53	0.03	0.02	0.92	0.02	0.00		0.04	0.04	0.05	0.87	0.00	0.18	0.79	0.00	0.01	0.01	0.23	0.01	0.01	0.04	0.71
0.34	0.55	0.05	0.04	0.86	0.04	0.00		0.06	0.05	0.09	0.80	0.01	0.18	0.79	0.00	0.02	0.01	0.27	0.01	0.02	0.08	0.63
0.36	0.56	0.08	0.05	0.80	0.07	0.00		0.06	0.05	0.15	0.73	0.01	0.18	0.78	0.00	0.02	0.01	0.31	0.01	0.02	0.11	0.55

$\mu_0$	$\mu$	$m_5 = f_0(1710)$						$R(m_2/m_1)$	$R(m_3/m_1)$	$R(m_4/m_1)$	$R(m_5/m_1)$	A	$\nu_1$	$\nu_2$	$\delta$	$\delta'$				
		$u + d$	$s$	$G_0$	$G_1$	$G_2$														
0.28	0.50	0.69	0.19	0.00	0.00	0.12		0.80		0.01		0.43		0.05		0.26	0.10	0.23	0.67	2.03
0.30	0.52	0.60	0.16	0.01	0.03	0.19		0.78		0.01		0.41		0.09		0.20	0.29	0.40	0.71	2.09
0.32	0.53	0.52	0.14	0.02	0.06	0.27		0.77		0.02		0.40		0.13		0.14	0.54	0.34	0.73	2.03
0.34	0.55	0.44	0.12	0.02	0.08	0.35		0.79		0.02		0.39		0.17		0.09	0.61	0.38	0.74	2.03
0.36	0.56	0.38	0.10	0.02	0.07	0.42		0.81		0.03		0.39		0.22		0.04	0.67	0.40	0.73	2.02

TABLE VI: The numerical analysis of the  $5 \times 5$  mixing in the  $0^{++}$  channel, with all 5 mass eigenstates ( $f_0(500)$ ,  $f_0(980)$ ,  $f_0(1370)$ ,  $f_0(1500)$ , and  $f_0(1710)$ ) as the input. Here  $a_0(980)$  is identified as the isotriplet partner.

$\mu_0$	$\mu$	$m_1 = f_0(500)$						$m_2 = f_0(980)$						$m_3 = f_0(1370)$						$m_4 = f_0(1500)$					
		$u+d$	$s$	$G_0$	$G_1$	$G_2$	$u+d$	$s$	$G_0$	$G_1$	$G_2$	$u+d$	$s$	$G_0$	$G_1$	$G_2$	$u+d$	$s$	$G_0$	$G_1$	$G_2$				
0.28	0.66	0.01	0.00	0.99	0.00	0.00	0.85	0.00	0.01	0.12	0.01	0.12	0.03	0.00	0.83	0.01	0.01	0.02	0.00	0.00	0.97				
0.30	0.69	0.07	0.00	0.92	0.00	0.00	0.85	0.00	0.07	0.00	0.08	0.00	0.00	0.00	1.00	0.00	0.08	0.09	0.00	0.00	0.83				
0.32	0.68	0.13	0.00	0.86	0.00	0.01	0.77	0.00	0.14	0.01	0.08	0.00	0.00	0.00	1.00	0.00	0.08	0.10	0.00	0.00	0.82				
0.34	0.68	0.20	0.01	0.78	0.00	0.01	0.69	0.00	0.21	0.02	0.08	0.02	0.00	0.00	0.97	0.01	0.09	0.11	0.00	0.00	0.81				
0.36	0.68	0.26	0.01	0.71	0.01	0.02	0.61	0.00	0.28	0.03	0.07	0.03	0.01	0.00	0.95	0.02	0.09	0.11	0.00	0.00	0.80				

$\mu_0$	$\mu$	$m_5 = f_0(1710)$						$R(m_2/m_1)$	$R(m_3/m_1)$	$R(m_4/m_1)$	$R(m_5/m_1)$	A	$\nu_1$	$\nu_2$	$\delta$	$\delta'$
		$u+d$	$s$	$G_0$	$G_1$	$G_2$										
0.28	0.66	0.01	0.95	0.00	0.03	0.01	0.12	0.49	0.48	0.01	0.08	0.39	-0.18	1.48	1.95	
0.30	0.69	0.01	0.90	0.00	0.01	0.09	0.13	0.62	0.44	0.03	0.04	0.02	-0.48	1.52	1.88	
0.32	0.68	0.01	0.89	0.00	0.00	0.09	0.21	0.66	0.46	0.04	0.03	0.50	0.10	1.46	1.83	
0.34	0.68	0.01	0.88	0.01	0.01	0.10	0.31	0.70	0.50	0.04	0.01	0.19	0.51	1.40	1.77	
0.36	0.68	0.01	0.87	0.01	0.01	0.10	0.42	0.76	0.54	0.05	0.00	0.25	0.53	1.34	1.71	

below 2 GeV (including  $f_0(500)$ ) and adopt (19) or (20) as the input, and treat  $\mu$  as a free parameter. But we need to impose one more constraint to fix the mass matrix completely.

To do that we may have to take into account that  $G_0$  is not an ordinary chromoball. There are two possibilities. If  $f_0(500)$  is the neuroball, it is natural to expect  $\nu_0$  to be of the same order as  $\nu_1$  and  $\nu_2$ . This must be clear from Fig. 7. In this case we may assume

$$\nu_0 \simeq \frac{\nu_1 + \nu_2}{2}. \quad (24)$$

On the other hand, if  $f_0(500)$  is the monoball, its coupling to ordinary quarkonia and chromoball states could be of second order. In this case  $\nu_0$  could be much smaller than  $\nu_1$  and  $\nu_2$ . Here we will use (24) as the constraint. Of course, we emphasize that there is no justification for this. We assume this just for simplicity to fix the mass matrix completely.

Now, with

$$G_0 = 4\mu_0^2, \quad G_1 = G_0 + \delta = 4\mu^2, \quad G_2 = G_0 + \delta', \quad (25)$$

we obtain Table V using (19), and Table VI using (20).

But diagonalizing the  $5 \times 5$  matrix involves solving a sixth order polynomial, and it is not easy to find the solution with the input data. So we have changed the input masses a bit, and used 550, 990, 1400, 1505, and 1722 MeVs for  $f_0(500)$ ,  $f_0(980)$ ,  $f_0(1370)$ ,  $f_0(1500)$ , and  $f_0(1710)$  to obtain Table V, and 550, 990, 1370, 1505, and 1800 for  $f_0(500)$ ,  $f_0(980)$ ,  $f_0(1370)$ ,  $f_0(1500)$ , and  $f_0(1710)$  to obtain Table VI.

Notice that here we have expressed  $G_0$  in terms of the neuron effective mass  $\mu_0$  (assuming that  $G_0$  is the neuroball) to compare it with the chromon mass  $\mu$  fixed by  $G_1$ . In this  $5 \times 5$  mixing the glueballs play the dominant role, because only two of the physical states can be the  $q\bar{q}$  states. So here the issue becomes which of the five physical states are the  $q\bar{q}$  states, not the glueball states.

Table V tells that  $f_0(1370)$  is predominantly the  $s\bar{s}$  state, and  $f_0(1710)$  becomes the mixed state about half of which is the  $u\bar{u} + d\bar{d}$  state (and  $f_0(1500)$  becomes the mixed states about quarter of which is the  $u\bar{u} + d\bar{d}$  state). This is consistent with Table I. Moreover, the table tells the followings. First,  $f_0(500)$  is the mainly the lowest energy glueball which could be interpreted as either the neuroball or the monoball. Second,  $f_0(980)$  and  $f_0(1500)$  are mainly the  $^1S_0$  and  $^5D_0$  chromoball states, and a considerable part of  $f_0(1710)$  is made of  $^5D_0$  chromoball.

In comparison Table VI tells that  $f_0(980)$  and  $f_0(1710)$  predominantly the  $u\bar{u} + d\bar{d}$  and  $s\bar{s}$  states, respectively. This is in line with Table II. Moreover, this table tells that  $f_0(500)$  is mainly the lowest energy the neuroball (or the monoball), and  $f_0(1370)$  and  $f_0(1500)$  are mainly the  $^1S_0$  and  $^5D_0$  chromoball states.

In the literature there have been diverse interpretations of the scalar mesons. One of the popular views is that  $f_0(500)$  and  $f_0(980)$  are the tetra-quark states [48–59], and  $f_0(1370)$  and  $f_0(1500)$  are the mixed states [60–62, 64–66]. Another view is that  $f_0(1370)$ ,  $f_0(1710)$ ,  $a_0(1450)$ , and  $K_0^*(1430)$  are the members of the flavor nonet,  $f_0(1710)$  being mainly the  $s\bar{s}$  state [67, 68]. In this view  $f_0(1500)$  can naturally be identified as predominantly the glueball state. And this seems to be endorsed by PDG [17].

Our analysis does not entirely support this. If we identify  $a_0(1450)$  as the isotriplet partner,  $f_0(1370)$  and  $f_0(1710)$  become the  $q\bar{q}$  states. But according to Table V,  $f_0(1370)$  turns out to be predominantly the  $s\bar{s}$  state. On the other hand Table VI shows that  $f_0(1710)$  becomes predominantly the  $s\bar{s}$  state, if we identify  $a_0(980)$  as the isotriplet partner. So, at this point it is premature to make a definite conclusion on which state,  $a_0(980)$  or  $a_0(1450)$ , is the isotriplet partner of the  $0^{++}$  isosinglet  $q\bar{q}$  state. We just remark that here our analysis does show that the possibility that  $a_0(980)$  could be the isotriplet partner remains an option.

But we like to emphasize two remarkable results of our mixing. First, both tables indicate that  $f_0(500)$  is

the neuroball. Moreover, they suggest that the neuron mass  $\mu_0$  is around 300 MeV, which is smaller than the chromon mass. This is interesting and reasonable. This should be compared with the popular view that  $f_0(500)$  (and  $f_0(980)$ ) are the tetra-quark states. As we have pointed out, in our quark and chromon model the tetra-quark states could be interpreted as the glueballs made of two neurons or chromons. This must be clear from Fig. 5 and Fig. 6. So this result is not inconsistent with the popular view that  $f_0(500)$  is a tetra-quark state.

Second, both tables suggest that  $f_0(1500)$  could be predominantly the chromoball state. This is very interesting. On the other hand, in both tables the radiative decay ratio  $R(f_0(1710)/f_0(1500))$  turns out to be too small compared to (21). But we notice that the relative radiative decay ratios in general are very sensitive to the inputs, so that this could be due to the *ad hoc* constraint (24).

## B. $2^{++}$ channel

In this channel we have three physical states below 2 GeV,  $f_2(1270)$ ,  $f_2'(1525)$ , and  $f_2(1950)$ . On the other hand we have to keep in mind that there is the fourth state  $f_2(2010)$  just above 2 GeV, which could better be included in the mixing. Another point is that PDG lists five more unestablished states,  $f_2(1430)$ ,  $f_2(1565)$ ,  $f_2(1640)$ ,  $f_2(1810)$ , and  $f_2(1910)$ , which could turn out to be real states. In this paper we will consider only the three plus  $f_2(2010)$  established states in the mixing analysis, but the fact that there are so many unestablished  $2^{++}$  states implies that we have to be careful to analyse this channel.

In the preceding paper we have studied the  $3 \times 3$  mixing of two quarkonia and one chromoball with

$$E = m^2(a_2), \quad a_2 = a_2(1320), \\ \Delta = 2(m^2(K^*) - m^2(a_2)), \quad K^* = K_2^*(1430), \quad (26)$$

and two physical states  $f_2(1270)$  and  $f_2(1950)$  as the input, and predicted the mass of the third physical state varying the chromon mass  $\mu$  as a free parameter [31]. The result suggests that, when the chromon mass  $\mu \simeq 760$  MeV,  $f_2(1270)$  becomes a mixture of  $u\bar{u} + d\bar{d}$  and chromoball,  $f_2(1950)$  becomes a mixture of  $u\bar{u} + d\bar{d}$ ,  $s\bar{s}$  and the chromoball, but  $f'(1525)$  becomes predominantly the  $s\bar{s}$  state. But when  $\mu$  becomes around 860 MeV,  $f_2(1270)$  becomes predominantly  $u\bar{u} + d\bar{d}$  state,  $f_2(1950)$  becomes predominantly the chromoball, and  $f_2'(1525)$  remains predominantly the  $s\bar{s}$  state. This was in line with the PDG suggestion, which interprets  $f_2(1270)$  and  $f_2'(1525)$  as the  $q\bar{q}$  states [17].

But now we have more experimental data on the  $J/\psi$  radiative decay from PDG [17]

$$J/\psi \rightarrow \gamma f_2(1270) \simeq (1.43 \pm 0.11) \times 10^{-3},$$

TABLE VII: The numerical analysis of the  $3 \times 3$  mixing in the  $2^{++}$  channel, with  $f_2(1270)$ ,  $f'_2(1525)$  and  $f_2(1950)$  as the input.

$\mu$	$m_1 = f'_2(1270)$			$m_2 = f'_2(1525)$			$m_3 = f_2(1950)$			$R(m_2/m_1)$	$R(m_3/m_1)$	$A$	$\nu$
	$u+d$	$s$	$G$	$u+d$	$s$	$G$	$u+d$	$s$	$G$				
0.92	0.86	0.01	0.13	0.04	0.88	0.07	0.10	0.10	0.80	0.41	2.33	0.07	0.79

TABLE VIII: The numerical analysis of the  $4 \times 4$  mixing in the  $2^{++}$  channel, with  $f_2(1270)$ ,  $f'_2(1525)$ ,  $f_2(1950)$ , and  $f_2(2010)$  as the input.

$\mu$	$m_1 = f_2(1270)$				$m_2 = f'_2(1525)$				$m_3 = f_2(1950)$				$m_4 = f_2(2010)$			
	$u+d$	$s$	$G$	$G'$	$u+d$	$s$	$G$	$G'$	$u+d$	$s$	$G$	$G'$	$u+d$	$s$	$G$	$G'$
0.90	0.80	0.01	0.19	0.00	0.06	0.85	0.09	0.00	0.13	0.14	0.72	0.01	0.01	0.00	0.01	0.99
0.91	0.79	0.01	0.18	0.02	0.06	0.85	0.08	0.01	0.09	0.09	0.67	0.15	0.05	0.05	0.07	0.83
0.92	0.79	0.01	0.17	0.03	0.06	0.85	0.07	0.01	0.06	0.06	0.61	0.27	0.09	0.08	0.14	0.69
0.93	0.79	0.01	0.16	0.04	0.06	0.86	0.07	0.01	0.03	0.03	0.54	0.39	0.12	0.10	0.22	0.55
0.94	0.78	0.01	0.16	0.04	0.06	0.86	0.07	0.02	0.01	0.01	0.44	0.53	0.14	0.12	0.33	0.41

$\mu$	$R(m_2/m_1)$	$R(m_3/m_1)$	$R(m_4/m_1)$	$A$	$\nu$	$\nu'$	$\delta$
0.90	1.49	1.43	0.37	0.11	0.89	0.14	1.16
0.91	1.62	1.26	0.34	0.14	0.91	0.44	0.94
0.92	1.71	1.13	0.33	0.15	0.93	0.56	0.75
0.93	1.78	1.04	0.31	0.17	0.96	0.62	0.56
0.94	1.82	0.98	0.31	0.18	0.99	0.62	0.39

$$J/\psi \rightarrow \gamma f'_2(1525) \simeq (4.5 + 0.7 - 0.4) \times 10^{-4},$$

$$J/\psi \rightarrow \gamma f_2(1950) \simeq (7.0 \pm 2.2) \times 10^{-4},$$

which give us

$$\begin{aligned} R(f_2(1525)/f_2(1270)) &\simeq 0.36, \\ R(f_2(1950)/f_2(1270)) &\simeq 0.49, \\ R(f_2(1950)/f'_2(1525)) &\simeq 1.56. \end{aligned} \quad (27)$$

So we could test these experimental data in our analysis.

In this paper we first do the  $3 \times 3$  mixing with all three inputs,  $f_2(1270)$ ,  $f'_2(1525)$ , and  $f_2(1950)$ , with (26). In this case we can fix all five mixing parameters, including the chromon mass  $\mu$ , completely. To find the solution, however, we have to vary the masses a bit. Changing the masses of  $f_2(1270)$ ,  $f'_2(1525)$ , and  $f_2(1950)$  to 1275, 1515, and 1944 MeVs, we obtain Table VII which suggests the chromon mass to be around 920 MeV.

One might worry that the chromon mass of Table VII,  $\mu \simeq 920$  MeV, is a bit too large. But remember that here the  $2^{++}$  chromoball is  $^5S_2$  state in which the spin of two chromons are parallel. And the spin-spin interaction could have made the chromon mass large. So the large chromon mass here actually includes the energy coming from the spin-spin interaction.

The result tells that  $f_2(1270)$  is predominantly the  $u\bar{u} + d\bar{d}$  state,  $f'_2(1525)$  is predominantly the  $s\bar{s}$  state, and

$f_2(1950)$  is predominantly the chromoball state. This agrees well with the result of the preceding paper, and is consistent with the PDG view [17, 31]. Notice that the table gives us  $R(f'_2(1525)/f_2(1270)) \simeq 0.41$  which agrees well with the PDG value 0.36, but  $R(f_2(1950)/f_2(1270))$  becomes 2.33 which is a little larger than the PDG value (27). But we find that we could reduce this number by changing the mass of  $f_2(1525)$  to around 1490 MeV. With this change of the input, the chromon mass is reduced to around 840 MeV and  $R(f_2(1950)/f_2(1270))$  becomes around 0.57.

Now, remember that here we have  $f_0(2010)$  just above 2 GeV, and it would be unfair to exclude this in the mixing. So we consider the  $4 \times 4$  mixing with the four mass eigenstates and (26) as the input, and obtain Table VIII. Here again we have changed the input masses a little, to 1275, 1500, 1944, and 2100 MeVs, to find the solution.

Remarkably the result in Table VIII is very similar to the Table VII. Although the numbers are different, the general feature is the same. Here again  $f_2(1270)$  becomes predominantly the  $u\bar{u} + d\bar{d}$  state,  $f'_2(1525)$  becomes predominantly the  $s\bar{s}$  state, and  $f_2(1950)$  becomes predominantly a chromoball state. The only new thing is that  $f_2(2010)$  becomes the second chromoball state, so that we can interpret  $f_2(1950)$  and  $f_2(2010)$  to be predominantly the  $^5S_2$  and  $^1D_2$  chromoballs.



TABLE IX: The numerical analysis of the  $4 \times 4$  mixing in the  $2^{++}$  channel, with states  $f_2(1270)$ ,  $f'_2(1525)$ ,  $f_2(1950)$  as the input. The fourth state could be interpreted as  $f_2(2010)$ .

$\mu$	$m_4$	$m_1 = f_2(1270)$				$m_2 = f'_2(1525)$				$m_3 = f_2(1950)$				$m_4$			
		$u+d$	$s$	$G$	$G'$	$u+d$	$s$	$G$	$G'$	$u+d$	$s$	$G$	$G'$	$u+d$	$s$	$G$	$G'$
0.90	2.86	0.80	0.01	0.19	0.00	0.06	0.85	0.09	0.00	0.14	0.14	0.72	0.00	0.00	0.00	0.00	0.99
0.91	2.11	0.79	0.01	0.18	0.02	0.06	0.85	0.08	0.01	0.09	0.09	0.68	0.14	0.05	0.05	0.06	0.84
0.92	2.07	0.79	0.01	0.18	0.02	0.06	0.85	0.08	0.01	0.05	0.05	0.54	0.36	0.10	0.09	0.21	0.61
0.93	2.07	0.79	0.01	0.18	0.03	0.06	0.86	0.07	0.01	0.02	0.02	0.42	0.54	0.13	0.11	0.33	0.43
0.94	2.08	0.78	0.01	0.17	0.03	0.06	0.86	0.07	0.01	0.01	0.01	0.33	0.65	0.14	0.12	0.43	0.21

$\mu$	$m_4$	$R(m_2/m_1)$	$R(m_3/m_1)$	$R(m_4/m_1)$	A	$\nu$	$\epsilon$
0.90	2.86	1.48	0.03	0.37	0.12	0.89	4.89
0.91	2.11	1.61	1.23	0.34	0.14	0.91	0.98
0.92	2.07	1.75	1.20	0.33	0.15	0.95	0.63
0.93	2.07	1.82	1.10	0.32	0.16	0.98	0.46
0.94	2.08	1.85	1.01	0.31	0.17	1.02	0.33

The main difference between the two tables is the  $J/\psi$  relative radiative decay ratio. This is because the ratio is very sensitive to the chromoball contents of the physical states, so that a small change of the chromoball contents influence the ratio significantly. In Table VIII the radiative decay ratios turn out to be larger than the PDG values (27). But we find that the ratios could be reduced to PDG values by changing the mass of  $f'_2(1525)$  to around 1490 MeV.

We can do the  $4 \times 4$  mixing with the three mass eigenstates below 2 GeV and (26) as the input, and try to predict the fourth state. The result is shown in Table IX. But here again we have changed the mass eigenvalues to 1275, 1500, and 1944 MeV to obtain the solutions. Remarkably it predicts that the mass of the fourth state is around 2100 MeV, which we can identify to be  $f_2(2010)$ . With this identification Table IX becomes very similar to Table VIII, which confirms that  $f_2(1270)$  is predominantly the  $u\bar{u} + d\bar{d}$  state,  $f'_2(1525)$  is predominantly the  $s\bar{s}$  state, but  $f_2(1950)$  and  $f_0(2010)$  are predominantly the  $^5S_2$  and  $^1D_2$  chromoballs.

So all in all the mixing in the  $2^{++}$  channel seems to work fine, and the upshot of our mixing is that  $f_2(1950)$  and  $f_0(2010)$  are predominantly the chromoball states. On the other hand, it is good to remember that there are different suggestions in the literature. Clearly there have been claims that  $f_2(1270)$  and  $f'_2(1525)$  are the  $q\bar{q}$  states as PDG suggests [72–74]. Moreover, there have been assertions that they can be viewed as molecular states [75–78].

Experimentally the situation is not better either, because here we have five unestablished states,  $f_2(1430)$ ,  $f_2(1565)$ ,  $f_2(1640)$ ,  $f_2(1810)$ , and  $f_2(1910)$  [17]. Some of them could turn out to be real states and make the mixing unreliable. So we need more time to understand

the  $2^{++}$  mixing more clearly.

### C. $0^{-+}$ channel

This channel has attracted special attention because of the octet-singlet mixing, the U(1) problem, PCAC etc. In this channel we have five established states below 2 GeV,  $\eta(548)$ ,  $\eta'(958)$ ,  $\eta(1295)$ ,  $\eta(1405)$ , and  $\eta(1475)$ , and one unestablished state  $\eta(1760)$ .

In the preceding paper we discussed the  $4 \times 4$  mixing with two  $q\bar{q}$  states and two chromoball states, one  $gg$  and one  $ggg$ , with

$$E = m^2(\pi), \quad \pi = \pi(140), \\ \Delta = 2(m^2(K) - m^2(\pi)), \quad K = K(498), \quad (28)$$

and  $\eta'(958)$ ,  $\eta(1405)$ , and  $\eta(1760)$  as the input. The result showed that the mass of the fourth physical state becomes around 550 MeV, which could be interpreted to be  $\eta(548)$ . In this case  $\eta(548)$  turns out to be a mixture of  $u\bar{u} + d\bar{d}$  and  $s\bar{s}$ , while  $\eta'(958)$  becomes predominantly a  $gg$  chromoball [31].

This was problematic and not in line with PDG, which interprets  $\eta'(958)$  as predominantly a  $q\bar{q}$  state. Moreover, the physical contents of  $\eta(1405)$  and  $\eta(1760)$  depended very much on the chromon mass. Another problem is that the  $J/\psi$  radiative decay ratios in this table do not agree well with PDG values. But a most critical defect of the  $4 \times 4$  mixing is that it can not explain all five physical states.

Moreover, experimentally PDG has new data which we have to explain

$$J/\psi \rightarrow \gamma\eta(548) \simeq (1.104 \pm 0.034) \times 10^{-3},$$

TABLE X: The numerical analysis of the  $5 \times 5$  mixing in the  $0^{-+}$  channel. Here we have used  $\eta'(958)$ ,  $\eta(1275)$ ,  $\eta(1405)$ ,  $\eta(1475)$ , and  $R(\eta(1475)/\eta'(958)) = 0.95$  as the input. The fifth state could be interpreted as  $\eta(548)$ .

$\mu$	$m_5$	$m_1 = \eta'(958)$						$m_2 = \eta(1295)$					$m_3 = \eta(1405)$					$m_4 = \eta(1475)$				
		$u + d$	$s$	$G_1$	$G_2$	$G_3$	$u + d$	$s$	$G_1$	$G_2$	$G_3$	$u + d$	$s$	$G_1$	$G_2$	$G_3$	$u + d$	$s$	$G_1$	$G_2$	$G_3$	
0.58	0.52	0.18	0.37	0.43	0.01	0.01	0.19	0.18	0.53	0.06	0.05	0.02	0.01	0.01	0.92	0.04	0.04	0.03	0.02	0.02	0.90	
0.58	0.52	0.18	0.36	0.44	0.01	0.00	0.17	0.16	0.50	0.15	0.02	0.05	0.04	0.04	0.82	0.05	0.02	0.02	0.01	0.02	0.93	
0.58	0.51	0.18	0.37	0.43	0.00	0.01	0.19	0.18	0.54	0.00	0.08	0.00	0.00	0.00	1.00	0.00	0.04	0.03	0.02	0.00	0.91	
0.58	0.52	0.17	0.35	0.46	0.02	0.00	0.14	0.13	0.44	0.30	0.00	0.12	0.10	0.10	0.68	0.00	0.00	0.00	0.00	0.00	1.00	

$\mu$	$m_5$	$m_5$					$R(m_2/m_1)$	$R(m_3/m_1)$	$R(m_4/m_1)$	$R(m_5/m_1)$	$A$	$\nu$	$\nu'$	$\delta$	$\delta'$	$\mu_0$
		$u + d$	$s$	$G_1$	$G_2$	$G_3$										
0.58	0.52	0.58	0.41	0.01	0.00	0.00	0.90	1.12	0.95	0.03	0.36	0.40	-0.17	0.62	-0.89	0.487
0.58	0.52	0.58	0.41	0.01	0.00	0.00	0.93	1.02	0.95	0.03	0.37	0.41	-0.17	0.58	-0.87	0.489
0.58	0.51	0.58	0.41	0.01	0.00	0.00	0.89	1.17	0.95	0.03	0.36	0.40	0.01	0.63	-0.91	0.485
0.58	0.52	0.57	0.42	0.01	0.01	0.00	0.97	0.84	0.95	0.03	0.38	0.43	-0.01	0.52	-0.85	0.492

$$\begin{aligned} J/\psi \rightarrow \gamma\eta'(958) &\simeq (5.15 \pm 0.16) \times 10^{-3}, \\ J/\psi \rightarrow \gamma\eta(1405/1475) &\simeq 4.9 \times 10^{-3}, \end{aligned} \quad (29)$$

which tells

$$\begin{aligned} R(\eta'(958)/\eta(548)) &\simeq 4.66, \\ R(\eta(1405/1475)/\eta(548)) &\simeq 4.44. \end{aligned} \quad (30)$$

So, in this paper we discuss the  $5 \times 5$  mixing which can explain all five established states.

Consider the following mixing matrix

$$M^2 = \begin{pmatrix} E + \frac{2}{3}\Delta & -\frac{\sqrt{2}}{3}\Delta & 0 & 0 & 0 \\ -\frac{\sqrt{2}}{3}\Delta & E + \frac{1}{3}\Delta + 3A & \nu_1 & \nu_2 & \nu_3 \\ 0 & \nu_1 & G_1 & 0 & 0 \\ 0 & \nu_2 & 0 & G_2 & 0 \\ 0 & \nu_3 & 0 & 0 & G_3 \end{pmatrix}, \quad (31)$$

which describes the mixing of two quarkonia and three chromoball states, two  $gg$  and one  $ggg$ , below 2 GeV. This has nine parameters. Now, normally we could choose seven inputs, (28) and five mass eigenvalue, and treat  $\mu$  as the free parameter. In this case we need one more constraint, and might impose the following constraint

$$\nu_1 = \nu, \quad \nu_2 = \frac{\nu_1 + \nu_3}{2}, \quad \nu_3 = \nu', \quad (32)$$

just for simplicity.

But here we choose a slightly different input. We choose four mass eigenstates,  $\eta'(958)$ ,  $\eta(1295)$ ,  $\eta(1405)$ ,  $\eta(1475)$ , and  $R(\eta(1475)/\eta'(958)) = 0.95$  of (30) in stead of  $\eta(548)$ . With this we could predict the mass of the fifth physical state. The reason is that, as we have pointed out the mathematical equations which we need to solve

to diagonalize the mass matrix are very rigid, so that we could not find the solution when we use the five mass eigenstates as the inputs. Assuming that  $G_3$  is the  $ggg$  chromoball we let

$$G_1 = 4\mu^2, \quad G_2 = 4\mu^2 + \delta, \quad G_3 = 9\mu^2 + \delta', \quad (33)$$

and obtain Table X using (32).

The result shows that the mass of the fifth physical state is around 520 MeV, which could be identified as  $\eta(548)$ . In this case  $\eta(548)$  turns out to be a mixture of  $u\bar{u} + d\bar{d}$  and  $s\bar{s}$ , while  $\eta'(958)$  becomes largely a mixture of  $s\bar{s}$  and a  $gg$  chromoball, with less than 20% contamination of  $u\bar{u} + d\bar{d}$ . And  $\eta(1295)$  is made of more than 50%  $gg$  chromoball and less than 20%  $u\bar{u} + d\bar{d}$  and  $s\bar{s}$  each. But remarkably, the table shows that  $\eta(1405)$  and  $\eta(1475)$  are mainly the  $gg$  and  $ggg$  chromoball states. Moreover, the  $J/\psi$  radiative decay ratios  $R(\eta(1405)/\eta'(958))$  is perfect, although  $R(\eta'(958)/\eta(548))$  looks a bit larger. This looks interesting and reasonable, considering the fact that we have imposed the *ad hoc* constraint (32).

Notice that  $\delta'$  in the table turn out to be negative, which tells that the mass of the three chromon bound state is smaller than the sum of the chromon mass. This implies that the binding of three chromons is quite strong. So in the table we have estimated the chromon mass  $\mu_0$  of the three chromons state, with  $G_3 = 9\mu_0^2$ .

Of course, we have different views in the literature. The popular view that PDG endorses is that  $\eta(548)$  and  $\eta'(958)$  are predominantly the  $u\bar{u} + d\bar{d}$  and  $s\bar{s}$  states, and that  $\eta(1295)$  and  $\eta(1475)$  are the first radial excitations of  $\eta(548)$  and  $\eta'(958)$  [79–81]. But it is widely agreed that  $\eta(1405)$  is indeed a pseudo-scalar glueball [82–88]. This is endorsed by PDG and by our analysis, although there exists a lattice result which might contradict with this view [11].

TABLE XI: The numerical analysis of the  $3 \times 3$  mixing in the  $0^{-+}$  channel. Here we choose  $\eta'(958)$  and  $\eta(1405)$  as the input and vary the mass of  $\eta(548)$  to obtain the table. No solution can be found when  $m(\eta(548)) > 541$  MeV.

$m(\eta(548))$	$A$	$\nu$	$\mu$	$m_1 = \eta(548)$			$m_2 = \eta'(958)$			$m_3 = \eta(1405)$			$R(m_3/m_2)$	$R(m_1/m_2)$
				$u+d$	$s$	$G$	$u+d$	$s$	$G$	$u+d$	$s$	$G$		
510	0.34	0.51	0.64	0.60	0.39	0.01	0.23	0.47	0.30	0.17	0.14	0.69	1.2	0.05
520	0.41	0.55	0.60	0.56	0.43	0.01	0.16	0.33	0.51	0.28	0.24	0.48	0.49	0.03
530	0.50	0.48	0.55	0.51	0.48	0.01	0.09	0.19	0.72	0.40	0.34	0.27	0.19	0.02
540	0.58	0.22	0.49	0.47	0.53	0.00	0.01	0.03	0.95	0.52	0.43	0.04	0.02	0.003

Our result implies that the spectrum of the light pseudo-scalar mesons could be understood within the context of the quarkonium-chromoball mixing. Nevertheless, the idea that  $\eta(1295)$  and  $\eta(1475)$  could be the radial excitations of  $\eta(548)$  and  $\eta'(958)$  should be taken seriously [79–81].

To see how this popular view fares in our quark and chromon model, we consider the  $3 \times 3$  mixing with only three physical states,  $\eta(548)$ ,  $\eta'(958)$ , and  $\eta(1405)$ , excluding the supposedly radially excited states  $\eta(1295)$  and  $\eta(1475)$ . Normally in the  $3 \times 3$  mixing we could use the three masses and (28) as the input to diagonalize the mass matrix, but in this case we could not find the solution. So we choose only two mass eigenvalues,  $\eta'(958)$  and  $\eta(1405)$ , and vary the mass of  $\eta(548)$ . With this we obtain Table XI.

Interestingly, when the mass of  $\eta(548)$  becomes 510 MeV, the radiative decay ratio  $R(\eta(1405)/\eta(958)) \simeq 1.2$  becomes close to the experimental value 0.95. In this case  $\eta(548)$  becomes 60%  $u\bar{u} + d\bar{d}$  and 39%  $s\bar{s}$ , but  $\eta'(958)$  becomes a mixture of 47%  $s\bar{s}$  and 30%  $g\bar{g}$ . And  $\eta(1405)$  becomes predominantly (69%) a chromoball.

To understand the physical meaning of Table XI, we notice that the physical contents depends very much on the mass of  $\eta(548)$ . Moreover, as the mass approaches to the physical value 548 MeV,  $\eta'(958)$  becomes predominantly the glueball. This is troublesome, and does not seem to support the PDG view (that  $\eta(1295)$  and  $\eta(1475)$  are the radial excitations of  $\eta(548)$  and  $\eta'(958)$ ) at all. This implies that our result shown in Table X is at least as good as the PDG view, although this matter has to be studied more carefully.

In this section we have extended and improved the numerical analysis of the quarkonium-chromoball mixing of the preceding paper in three channels  $0^{++}$ ,  $2^{++}$ , and  $0^{-+}$  below 2 GeV, based on our quark and chromon model. Although the numerical results are still inconclusive, the results in this paper seem to work better.

Theoretically it must be clear that the numerical mixing should be regarded as an approximation. Moreover, technically the equation we need to solve to diagonalize the mass matrix is very rigid and sensitive to the *ad hoc*

constraints we have imposed. With these shortcomings it is natural that our results are not perfect. Nevertheless, it is fair to say that the above mixing analysis does show that the quark and chromon model provides a conceptually simple way to understand the glueballs and their mixing with quarkonia.

## VI. DISCUSSIONS

One of the main problems in hadron spectroscopy has been the identification of the glueballs. In this paper we have made the numerical quarkonium-glueball mixing analysis to identify the glueballs, based on the quark and chromon model [31]. Our mixing analysis confirms that the glueballs (i.e., the chromoballs) play the fundamental role in the hadron spectroscopy, although in general (except for the oddballs) they exist as mixed states. In fact the analysis tells that it is simply impossible to understand the meson spectroscopy without them.

Of course there are other models of glueball, in particular the constituent gluon model, which allow similar mixing analysis. In fact, superficially our mixing analysis is almost identical to the mixing in this model. As we have emphasized, however, the constituent model has the critical defect that it can not tell exactly what are the constituent gluons. In comparison our model clearly tell what are the constituent gluons and what are the binding gluons which bind the constituent gluons. This is because our model is based on different logic, that QCD is made of two types of gluons which play different roles. No other model is based on this fact.

To amplify this point consider the so-called “model independent” calculations of gluball spectrum, the QCD sum rule approach [6] and the lattice calculation [10, 11]. It has been assumed that these calculations are based on the first principles of QCD and thus regarded as model independent. But we have to know what is the first principles of QCD before we know how to calculate the glueball spectrum according to the principles. In the QCD sum rule approach we have two ways to calculate the glueball mass, with the gauge invariant current operators made of two chromons or the conventional current

operators made of two field strengths. And obviously the two methods will give us different results.

Exactly the same way, in the lattice calculation we can construct the glueballs implementing the Abelian decomposition on lattice or without implementing it. And again we get different results [26, 27]. These two examples clearly tell that we must understand the first principles of QCD first, before we actually make the “model independent” calculations. As we have explained in the first part of the paper, the Abelian decomposition allows us to do that. And this is not a conjecture, but mathematically a well established fact in QCD [20–30, 41–44]. This is the advantage of our model.

Our analysis was able to pinpoint the glueball candidates below 2 GeV successfully. Indeed our result strongly indicates that  $f_0(500)$  and  $f_0(1500)$  in the  $0^{++}$  sector,  $f_2(1950)$  in the  $2^{++}$  sector, and  $\eta(1405)$  and  $\eta(1475)$  in the  $0^{-+}$  sector become predominantly the glueballs. Some of them have been suggested to be the glueball states before, but some of them (e.g.,  $f_0(500)$  and  $\eta(1475)$ ) are our suggestion.

In our mixing analysis we have also tried to settle other unresolved issues. First, in the  $0^{++}$  sector an important issue is what is the isotriplet  $q\bar{q}$  partner of the isosinglet  $q\bar{q}$ . There are two contending views. The popular view endorsed by PDG is that  $a_0(1450)$  is the isotriplet partner, but the opposite view suggests that  $a_0(980)$  is the isotriplet partner [17]. The popular view appears intuitively strange because, if this is so, the strange flavor octet partner  $K_0^*(1430)$  becomes lighter than  $a_0(1450)$ . So it is important to find out which view is correct, and why. We tried to resolve this issue in our mixing. Unfortunately our analysis could not provide a conclusive answer on this, but it does imply that the opposite view is not completely excluded yet.

Another issue in this sector is whether the neurons could form a bound state or not. Our result indicates that they could. In fact, our analysis suggests that  $f_0(500)$  could be such a neuroball state. And this is independent of which state we choose to be the isotriplet partner. In our quark and chromon model the neuroballs (if exist) should look very much like loosely bound states of two (or three)  $q\bar{q}$  mesons or  $gg$  chromoballs, and  $f_0(500)$  nicely fits in this picture. Remarkably, this is consistent with the popular view advocated by many authors [48–54]. But we emphasize that in detail two views are different. The one interprets  $f_0(500)$  to be a glueball, but the other interprets it a molecular state.

A related issue is whether the monopole condensation in QCD could create a  $0^{++}$  vacuum fluctuation mode or not [20, 21, 31]. Theoretically this, of course, is a fundamental question. If the answer turns out to be in the affirmative,  $f_0(500)$  would be a natural candidate of the vacuum fluctuation. But our analysis could not provide a definite answer on this, and this possibility remains open.

The mixing in the  $2^{++}$  sector is rather straightforward because there are no controversial issues here. Here we have three physical states below 2 GeV, and our result tells that  $f_2(1275)$  and  $f_2'(1525)$  are the  $u\bar{u} + d\bar{d}$  and  $s\bar{s}$  states, respectively. This, of course, is in line with the PDG interpretation [17]. Moreover, our result tells that  $f_2(1950)$  is predominantly the chromoball state, which agrees with our result in the preceding paper [31].

This sounds all very nice, but we have to swallow this with a grain of salt. The problem is that in this sector PDG shows that there are five unestablished states, and some of them could turn out to be real. And it is quite possible that this could give us a serious trouble.

Finally, in the  $0^{-+}$  sector an important issue is whether  $\eta(1295)$  and  $\eta(1750)$  are the radial excitations of  $\eta(548)$  and  $\eta'(958)$  or not [79–81]. Our mixing analysis provides a different picture. Our result tells that  $\eta(1295)$  can be viewed as a mixed state made of more than 50%  $gg$  chromoball and less than 20%  $u\bar{u} + d\bar{d}$  and  $s\bar{s}$  each, and  $\eta(1475)$  is mainly the  $ggg$  chromoball state. This looks very interesting and reasonable, although we have yet to see which view is correct.

One of the problems in the mixing analysis is that the mathematical equations to diagonalize the mass matrix are very rigid and sensitive to the input data, but in reality we often do not have enough input data. This has forced us to impose *ad hoc* constraints like (24) and (32) which may have distorted the reality. But this is a technical problem we could avoid when enough experimental data become available.

Independent of the details, however, we emphasize the conceptual simplicity and clarity of the quark and chromon model. As a natural generalization of the quark model it tells what are the glueballs made of and how they mix with quarkonia without ambiguity. Most importantly, it provides us the general framework of the hadron spectroscopy in simple and clear terms.

Obviously our numerical results in this paper are not perfect, and can not explain everything. Nevertheless they do demonstrate that the quark and chromon model is at least as good as any other model in the literature which describes the glueballs and their mixing with quarkonia. Moreover, the numerical mixing analysis is not the only the application of our model. The next application would be to implement the Abelian decomposition to the QCD sum rule and the lattice QCD calculations, and obtain a better understanding of glueballs. The work in these directions are in progress.

## APPENDIX

The Weyl group or Weyl reflection group of  $SU(N)$  is the symmetric group  $S_N$  of degree  $N$ , the permutation group of  $N$  elements. For  $SU(2)$ , the Weyl group consists

of two elements

$$W_1 = \begin{pmatrix} 1 & 0 \\ 0 & 1 \end{pmatrix}, \quad W_2 = \begin{pmatrix} 0 & 1 \\ -1 & 0 \end{pmatrix}. \quad (34)$$

For SU(3), the Weyl group is the permutation group of three elements which consists of six elements,

$$\begin{aligned} W_1 &= \begin{pmatrix} 1 & 0 & 0 \\ 0 & 1 & 0 \\ 0 & 0 & 1 \end{pmatrix}, & W_2 &= \begin{pmatrix} 0 & 1 & 0 \\ -1 & 0 & 0 \\ 0 & 0 & 1 \end{pmatrix}, \\ W_3 &= \begin{pmatrix} 1 & 0 & 0 \\ 0 & 0 & 1 \\ 0 & -1 & 0 \end{pmatrix}, & W_4 &= \begin{pmatrix} 0 & 0 & 1 \\ 0 & 1 & 0 \\ -1 & 0 & 0 \end{pmatrix}, \\ W_5 &= \begin{pmatrix} 0 & -1 & 0 \\ 0 & 0 & 1 \\ -1 & 0 & 0 \end{pmatrix}, & W_6 &= \begin{pmatrix} 0 & 0 & 1 \\ -1 & 0 & 0 \\ 0 & -1 & 0 \end{pmatrix}. \end{aligned} \quad (35)$$

Obviously the above matrices are the elements of SU(2) and SU(3) which satisfy  $W_a W_a^\dagger = 1$  and  $\det W_a = 1$ , so that they form a subgroup of SU(2) and SU(3).

The color reflection group is a generalization of the Weyl group. For SU(2), the reflection group is made of four elements

$$\begin{aligned} R_1 &= \begin{pmatrix} 1 & 0 \\ 0 & 1 \end{pmatrix}, & R_2 &= \begin{pmatrix} 0 & 1 \\ -1 & 0 \end{pmatrix}, \\ R_3 &= \begin{pmatrix} -1 & 0 \\ 0 & -1 \end{pmatrix}, & R_4 &= \begin{pmatrix} 0 & -1 \\ 1 & 0 \end{pmatrix}, \end{aligned} \quad (36)$$

which can be expressed by

$$R_k = w_a W_b, \quad (a = 1, 2; \quad b = 1, 2; \quad k = 1, 2, \dots, 4),$$

$$w_1 = \begin{pmatrix} 1 & 0 \\ 0 & 1 \end{pmatrix}, \quad w_2 = \begin{pmatrix} -1 & 0 \\ 0 & -1 \end{pmatrix}. \quad (37)$$

For SU(3) the color reflection group is made of 24 elements which can be expressed by

$$\begin{aligned} R_k &= w_a W_b, \\ (a &= 1, 2, 3, 4; \quad b = 1, 2, \dots, 6; \quad k = 1, 2, \dots, 24), \\ w_1 &= \begin{pmatrix} 1 & 0 & 0 \\ 0 & 1 & 0 \\ 0 & 0 & 1 \end{pmatrix}, & w_2 &= \begin{pmatrix} 1 & 0 & 0 \\ 0 & -1 & 0 \\ 0 & 0 & -1 \end{pmatrix}, \\ w_3 &= \begin{pmatrix} -1 & 0 & 0 \\ 0 & 1 & 0 \\ 0 & 0 & -1 \end{pmatrix}, & w_4 &= \begin{pmatrix} -1 & 0 & 0 \\ 0 & -1 & 0 \\ 0 & 0 & 1 \end{pmatrix}, \end{aligned} \quad (38)$$

where  $W_b$  are the elements of SU(3) Weyl group.

The importance of the color reflection group comes from the fact that it becomes the residual symmetry of the color gauge group after the Abelian decomposition, so that it plays the role of the color gauge symmetry after the decomposition. This means that the color reflection invariance assures the gauge invariance in QCD, and thus plays a fundamental role in hadron spectroscopy [20, 21].

## ACKNOWLEDGEMENT

The work is supported in part by the National Natural Science Foundation of China (Grants 11575254, 11447105, and 11475227), Chinese Academy of Sciences Visiting Professorship for Senior International Scientists (Grant 2013T2J0010), China Scholarship Council, Basic Science Research Program through the National Research Foundation of Korea (NRF) funded by the Ministry of Education (Grants 2015-R1D1A1A0-1057578 and 2015-R1D1A1A0-1059407), and by Konkuk University.

- 
- [1] H. Fritzsch and P. Minkowski, *Nuovo Cimento* **30A**, 393 (1975).
  - [2] P. G. O. Freund and Y. Nambu, *Phys. Rev. Lett.* **34**, 1645 (1975).
  - [3] J. Kogut, D. Sinclair, and L. Susskind, *Nucl. Phys.* **B114**, 199 (1976).
  - [4] R. L. Jaffe and K. Johnson, *Phys. Lett.* **B60**, 201 (1976).
  - [5] P. Roy and T. Walsh, *Phys. Lett.* **B78**, 62 (1978).
  - [6] M. Shifman, A. Vainshtein, and V. Zakharov, *Nucl. Phys.* **B147**, 385 (1979).
  - [7] J. Coyne, P. Fishbane, and S. Meshkov, *Phys. Lett* **B91**, 259 (1980).
  - [8] M. Chanowitz, *Phys. Rev. Lett.* **46**, 981 (1981).
  - [9] J. Cornwall and A. Soni, *Phys. Lett.* **B120**, 431 (1983).
  - [10] G. Bali *et al.* [UKQCD Collaboration], *Phys. Lett.* **B309**, 378 (1993).
  - [11] C. Morningstar and M. Peardon, *Phys. Rev.* **D60**, 034509 (1999).
  - [12] C. Amsler and N. Tornqvist, *Phys. Rep.* **389**, 61 (2004).
  - [13] D. V. Bugg, *Phys. Rep.* **397**, 61 (2004).
  - [14] E. Klempt and A. Zaitsev, *Phys. Rep.* **454**, 1 (2007).
  - [15] V. Mathieu, N. Kochelev, and V. Vento, *Int. J. Mod. Phys.* **E18**, 1 (2009).
  - [16] W. Ochs, *J. Phys.* **G40**, 043001 (2013).
  - [17] K. Olive *et al.*, [Particle Data Group], *Review of Particle Physics*, *Chin. Phys.* **C38**, 090001 (2014).
  - [18] J. Dudek *et al.*, *Eur. Phys. J.* **A48**, 187 (2012).
  - [19] D. Dutta *et al.* [PANDA Collaboration], *Nucl. Phys.* **A862**, 231 (2011).
  - [20] Y. M. Cho, *Phys. Rev.* **D21**, 1080 (1980).
  - [21] Y. M. Cho, *Phys. Rev. Lett.* **46**, 302 (1981).
  - [22] Y. M. Cho, *Phys. Rev.* **D23**, 2415 (1981).
  - [23] Y. S. Duan and M. L. Ge, *Sci. Sinica* **11**, 1072 (1979).
  - [24] S. Kato, K. Kondo, T. Murakami, A. Shibata, T. Shinohara, and S. Ito, *Phys. Lett.* **B632**, 326 (2006).
  - [25] S. Ito, S. Kato, K. Kondo, T. Murakami, A. Shibata, and T. Shinohara, *Phys. Lett.* **B645**, 67 (2007).
  - [26] N. Cundy, Y. M. Cho, W. Lee, and J. Leem, *Phys. Lett.*

- B729**, 192 (2014).
- [27] N. Cundy, Y. M. Cho, W. Lee, and J. Leem, Nucl. Phys. **B895**, 64 (2015).
  - [28] W. S. Bae, Y. M. Cho, and S. W. Kimm, Phys. Rev. **D65**, 025005 (2001).
  - [29] Y. M. Cho, Franklin H. Cho, and J. H. Yoon, Phys. Rev. **D87**, 085025 (2013).
  - [30] Y. M. Cho, Int. J. Mod. Phys. **A29**, 1450013 (2014).
  - [31] Y. M. Cho, X. Y. Pham, Pengming Zhang, Ju-Jun Xie, and Li-Ping Zou, Phys. Rev. **D91**, 114020 (2015). Notice that Table IV in this paper has a typological error which is corrected in Table I in the present paper.
  - [32] J. Schwinger, Phys. Rev. **82**, 664 (1951).
  - [33] Y. M. Cho and D. G. Pak, Phys. Rev. Lett. **86**, 1947 (2001); **91**, 039151.
  - [34] W. S. Bae, Y. M. Cho, and D. G. Pak, Phys. Rev. **D64**, 017303 (2001).
  - [35] D. Gross and F. Wilczek, Phys. Rev. Lett. **30**, 1343 (1973).
  - [36] H. Politzer, Phys. Rev. Lett. **30**, 1346 (1973).
  - [37] V. Schanbacher, Phys. Rev. **D26**, 489 (1982).
  - [38] Y. M. Cho and D. G. Pak, Phys. Rev. **D65**, 074027 (2002).
  - [39] Y. M. Cho, M. L. Walker, and D. G. Pak, JHEP **05**, 073 (2004).
  - [40] Y. M. Cho, Phys. Rev. Lett. **44**, 1115 (1980).
  - [41] L. Faddeev and A. Niemi, Phys. Rev. Lett. **82**, 1624 (1999).
  - [42] S. Shabanov, Phys. Lett. **B458**, 322 (1999); **B463**, 263 (1999).
  - [43] H. Gies, Phys. Rev. **D63**, 125023 (2001).
  - [44] R. Zucchini, Int. J. Geom. Meth. Mod. Phys. **1**, 813 (2004).
  - [45] Y. M. Cho, Phys. Lett. **B115**, 125 (1982).
  - [46] K. Kondo, S. Kato, A. Shibata, and T. Shinohara, Phys. Rep. **579**, 1 (2015).
  - [47] See for example, M. Peskin and D. Schroeder, *An Introduction to Quantum Field Theory* (Addison-Wesley) 1995.
  - [48] H. Nagahiro and A. Hosaka, Phys. Rev. **C88**, 055203 (2003).
  - [49] M. Napsuciale and S. Rodriguez, Phys. Rev. **D70**, 094043 (2004).
  - [50] J. R. Pelaez and G. Rios, Phys. Rev. Lett. **97**, 242002 (2006).
  - [51] H.-X. Chen, A. Hosaka, and S.-L. Zhu, Phys. Lett. **B650**, 369 (2007).
  - [52] F. Giacosa, Phys. Rev. **D75**, 054007 (2007).
  - [53] J. T. Londergan, J. Nebreda, J. Pelaez, and A. Szczepaniak, Phys. Lett. **B729**, 9 (2014).
  - [54] A. H. Fariborz, J. Schechter, S. Zarepour, and M. Zebarjad, Phys. Rev. **D90**, 033009 (2014).
  - [55] M. Alford and R. Jaffe, Nucl. Phys. **B578**, 367 (2000).
  - [56] L. Maiani, F. Piccinini, A. Polosa, and V. Riquer, Phys. Rev. Lett. **93**, 212002 (2004).
  - [57] H. J. Lee and N. I. Kochelev, Phys. Lett. **B642**, 358 (2006).
  - [58] L. Maiani, A. D. Polosa, and V. Riquer, Phys. Lett. **B651**, 129 (2007).
  - [59] H. J. Lee, N. I. Kochelev, and Y. Oh, Phys. Rev. **D87**, 117901 (2013).
  - [60] F. E. Close, A. Kirk, Phys. Lett. **B483**, 345 (2000).
  - [61] M. Ablikim, et al. [BES Collaboration], Phys. Lett. **B607**, 243 (2005).
  - [62] F. Giacosa, Th. Gutsche, V. E. Lyubovitskij, and A. Faessler, Phys. Rev. **D72**, 094006 (2005).
  - [63] D. Parganlija, F. Giacosa, D. Rischke, Phys. Rev. **D82**, 054024 (2010).
  - [64] A. Fariborz, A. Azizi, and A. Asrar, Phys. Rev. **D91**, 073013 (2015).
  - [65] A. Kirk, Phys. Lett. **B489**, 29 (2000).
  - [66] A. Fariborz, A. Azizi, and A. Asrar, Phys. Rev. **D92**, 113003 (2015).
  - [67] C. Amsler and F. Close, Phys. Rev. **D53**, 295 (1996).
  - [68] F. Close and A. Kirk, Euro. Phys. J. **C21**, 531 (2001).
  - [69] W. J. Lee and D. Weingarten, Phys. Rev. **D61**, 014015 (2000).
  - [70] S. Janowski, F. Giacosa, and D. H. Rishke, Phys. Rev. **D90**, 114005 (2014).
  - [71] F. Brunner and A. Rebhan, Phys. Rev. Lett. **115**, 131601 (2015).
  - [72] D. M. Li, H. Yu, and Q. X. Shen, J. Phys. G: Nucl. Part. Phys. **27**, 807 (2001).
  - [73] F. Giacosa, T. Gutsche, V. E. Lyubovitskij, and A. Faessler, Phys. Rev. **D72**, 114021 (2005).
  - [74] Zao-Chen Ye, Xiao Wang, Xiang Liu, Qiang Zhao, Phys. Rev. **D86**, 054025 (2012).
  - [75] R. Molina, D. Nicmorus, and E. Oset, Phys. Rev. **D78**, 114018 (2008).
  - [76] C. Garcia-Recio, L. S. Geng, J. Nieves, L. Salcedo, E. Wang, and J. J. Xie, Phys. Rev. **D87**, 096006 (2013).
  - [77] Ju-Jun Xie, E. Oset, Eur. Phys. J. **A51**, 111 (2015).
  - [78] Ju-Jun Xie, E. Oset, and Li-Sheng Geng, Phys. Rev. **C93**, 025202 (2016).
  - [79] F. Close and A. Kirk, Phys. Lett. **B397**, 333 (1997).
  - [80] T. Barnes, F. Close, P. Page, and E. Swanson, Phys. Rev. **D55**, 4157 (1997).
  - [81] T. Gutsche, V. Lyubovitskij, and M. Tichy, Phys. Rev. **D79**, 014036 (2009).
  - [82] M. Acciarri et al. [L3 collaboration], Phys. Lett. **B501**, 1 (2001).
  - [83] F. Close, G. Farrar, and Z. Li, Phys. Rev. **D55**, 5749 (1997).
  - [84] D. M. Li, H. Yu, and S. S. Fang, Eur. Phys. J. **C28**, 335 (2003).
  - [85] L. Faddeev, A. Niemi, and U. Wieder, Phys. Rev. **D70**, 114033 (2004).
  - [86] M. Majewski, J. Phys. G: Nucl. Part. Phys. **38**, 035008 (2011).
  - [87] Feng Wang, Junlong Chen, and Jueping Liu, Phys. Rev. **D92**, 076004 (2015).
  - [88] Hai-Yang Cheng, Hsiang-Nan Li, and Keh-Fei Liu, Phys. Rev. **D79**, 014024 (2009).